The magnetic acceleration/collimation paradigm for relativistic jets

Nektarios Vlahakis
University of Athens

outline

- introduction: astrophysical jets
- the MHD description
  - ⋆ acceleration – collimation
  - ⋆ models (semi-analytical – simulations)

Jets from Young Stars

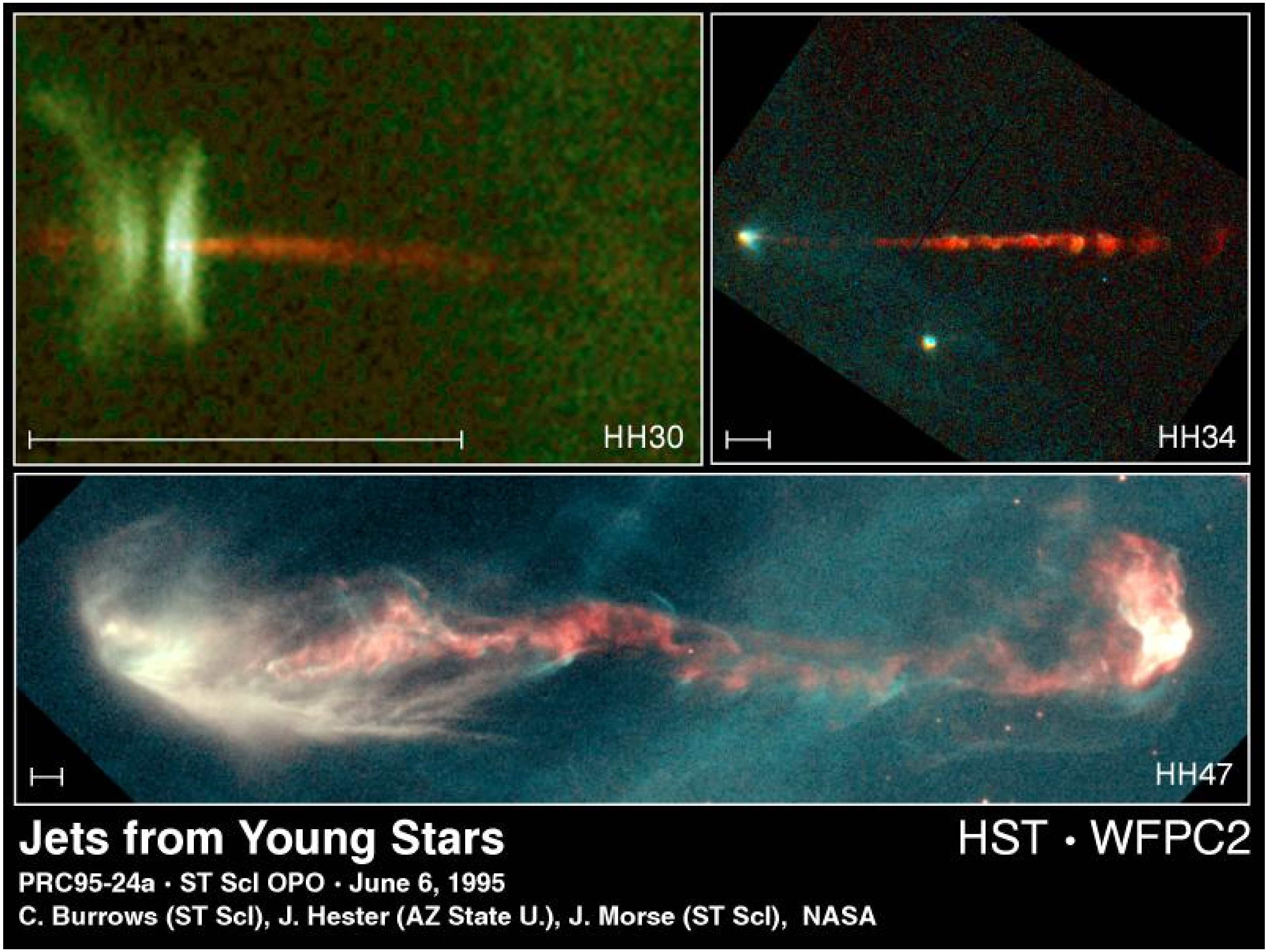

(scale =1000 AU, $V_\infty = a few 100$km/s)

Jets from Active Galactic Nuclei

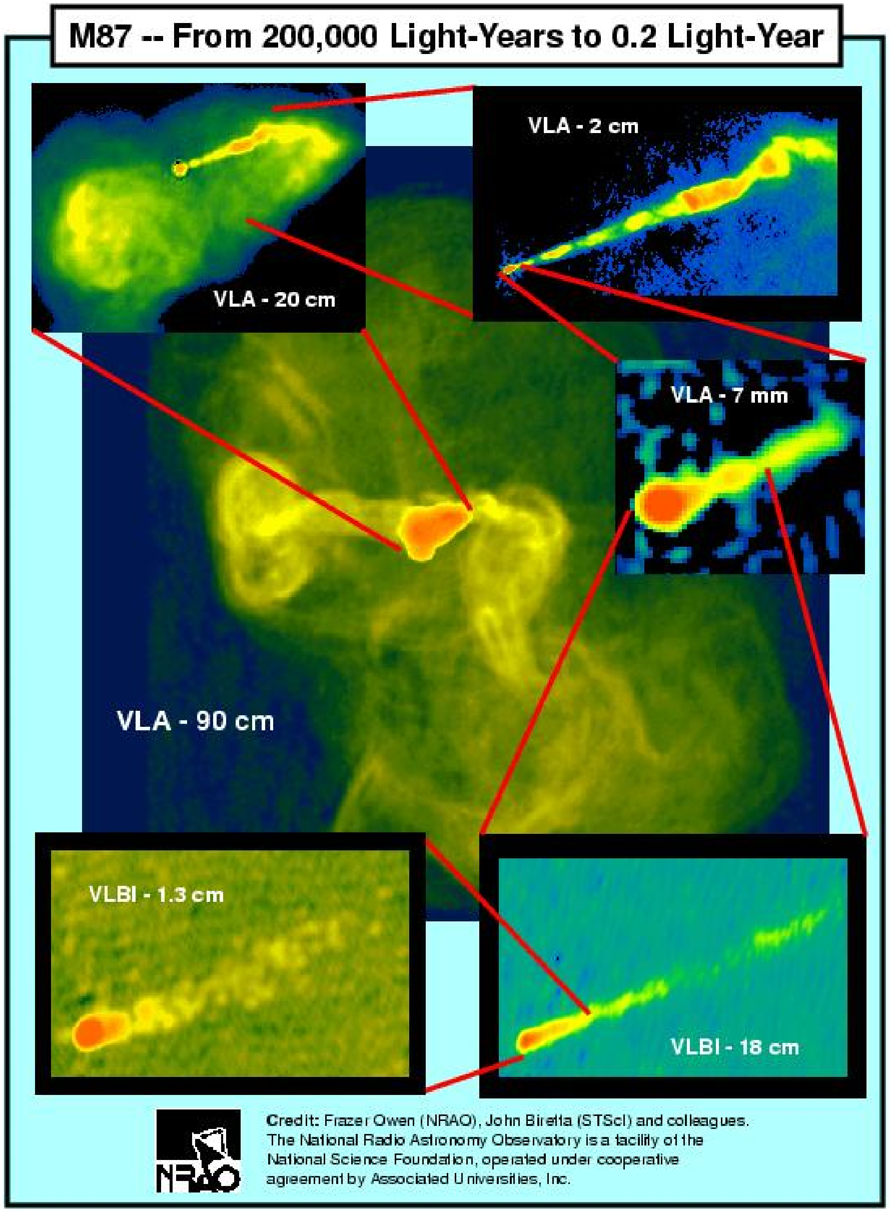

Jets from Active Galactic Nuclei

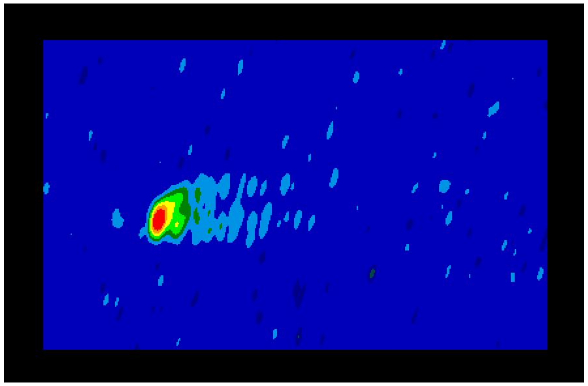

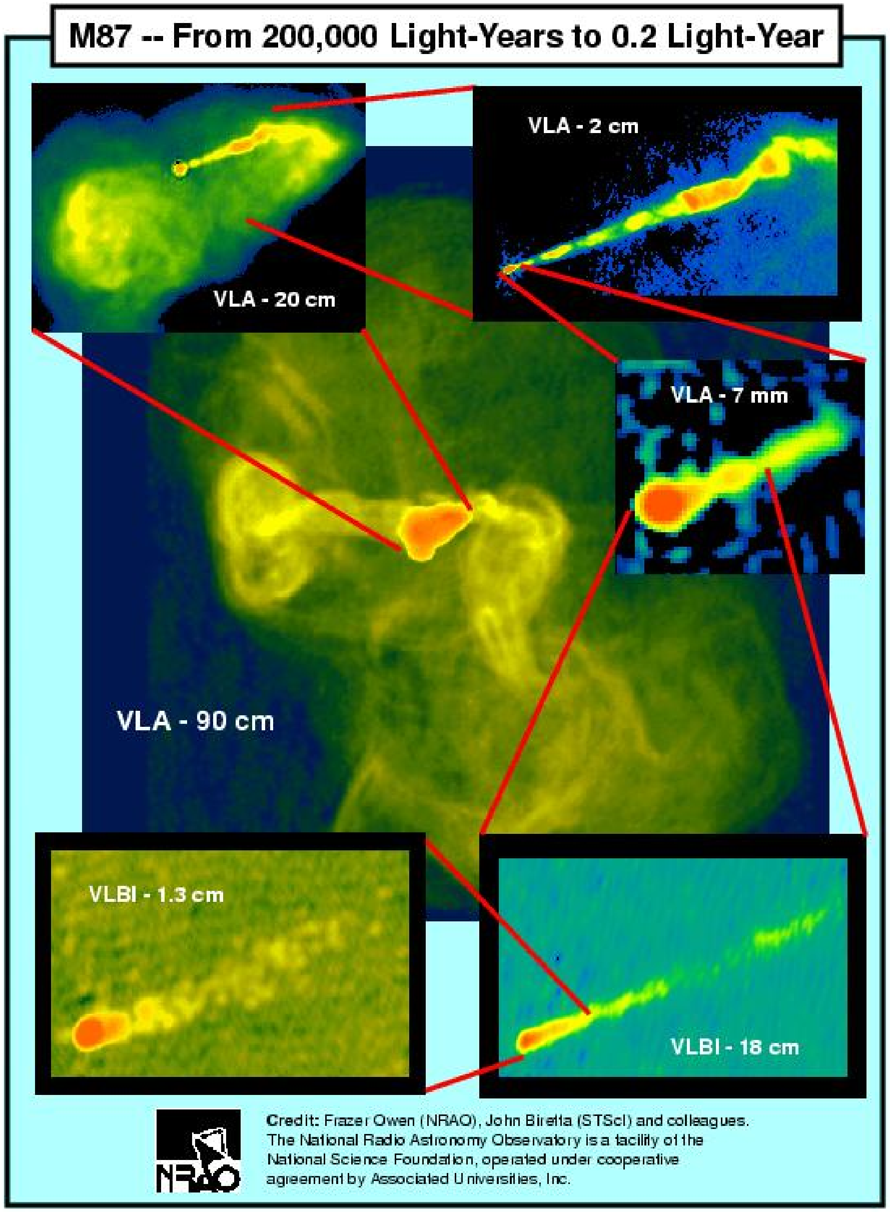

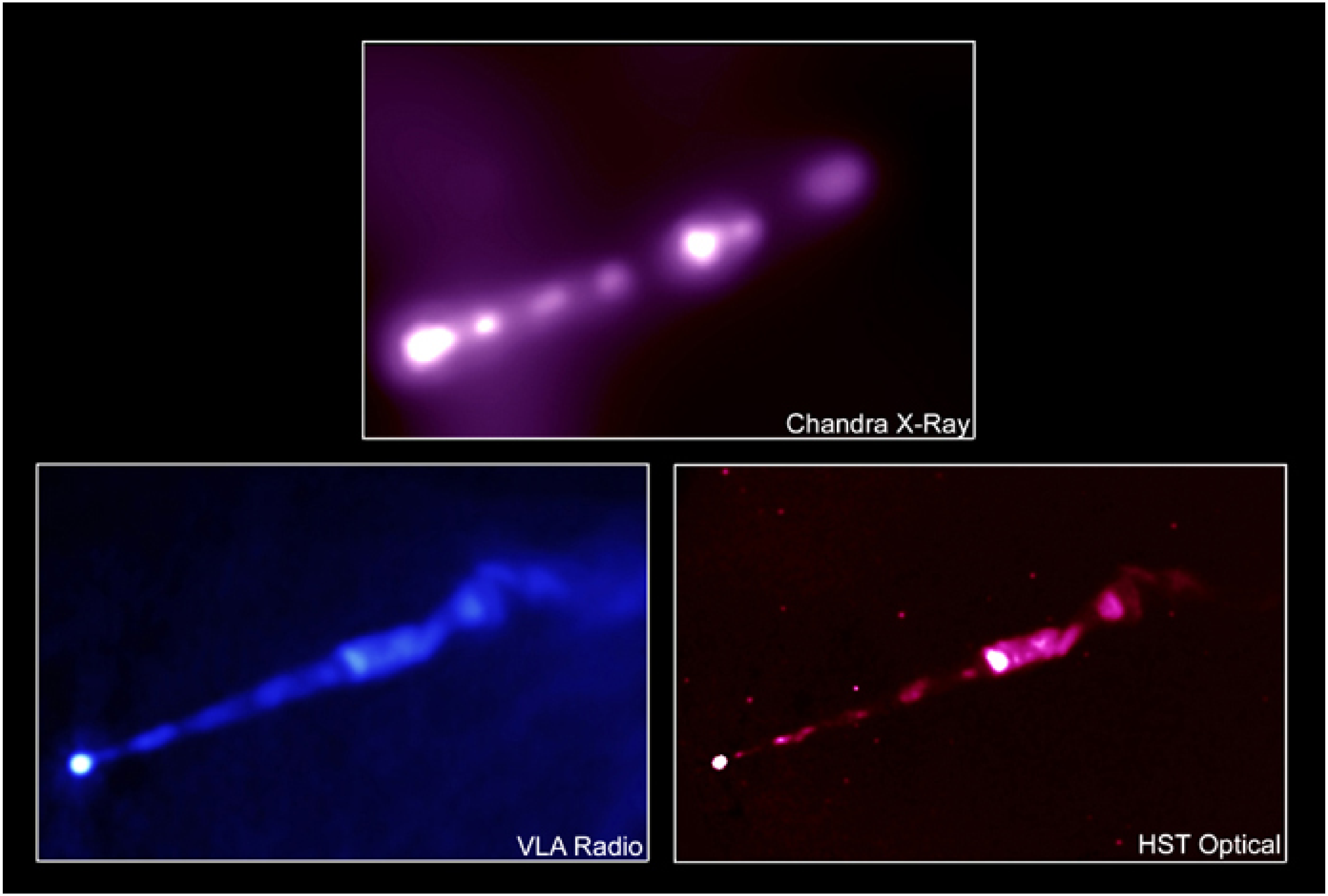
Chandra X-Ray
VLA Radio
HST Optical

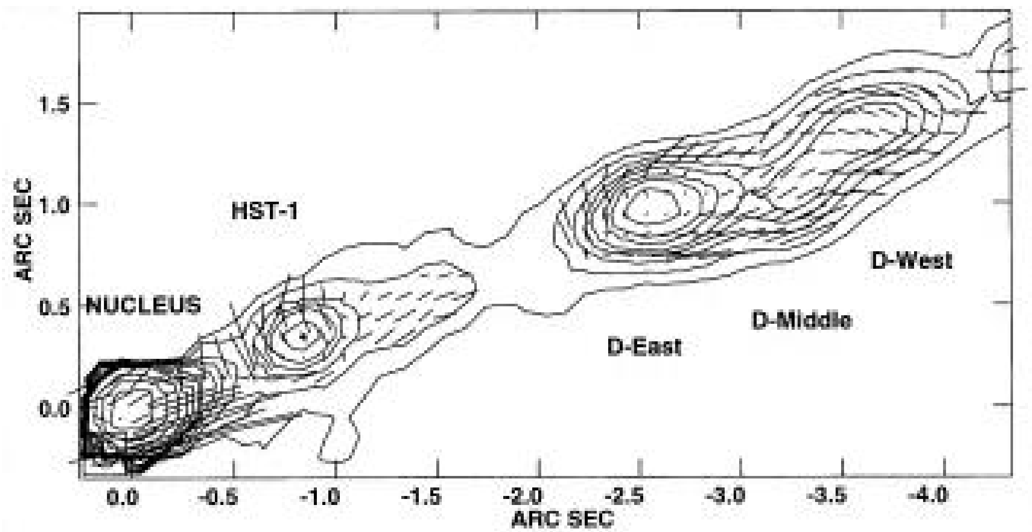

M87 - OPTICAL POLARIZATION

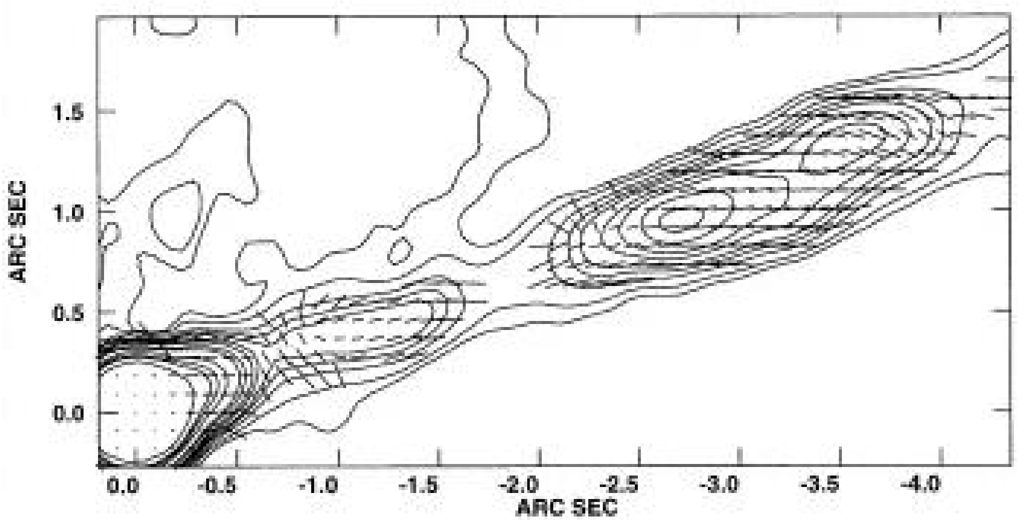

M87 - RADIO POLARIZATION

Superluminal Motion in the M87 Jet

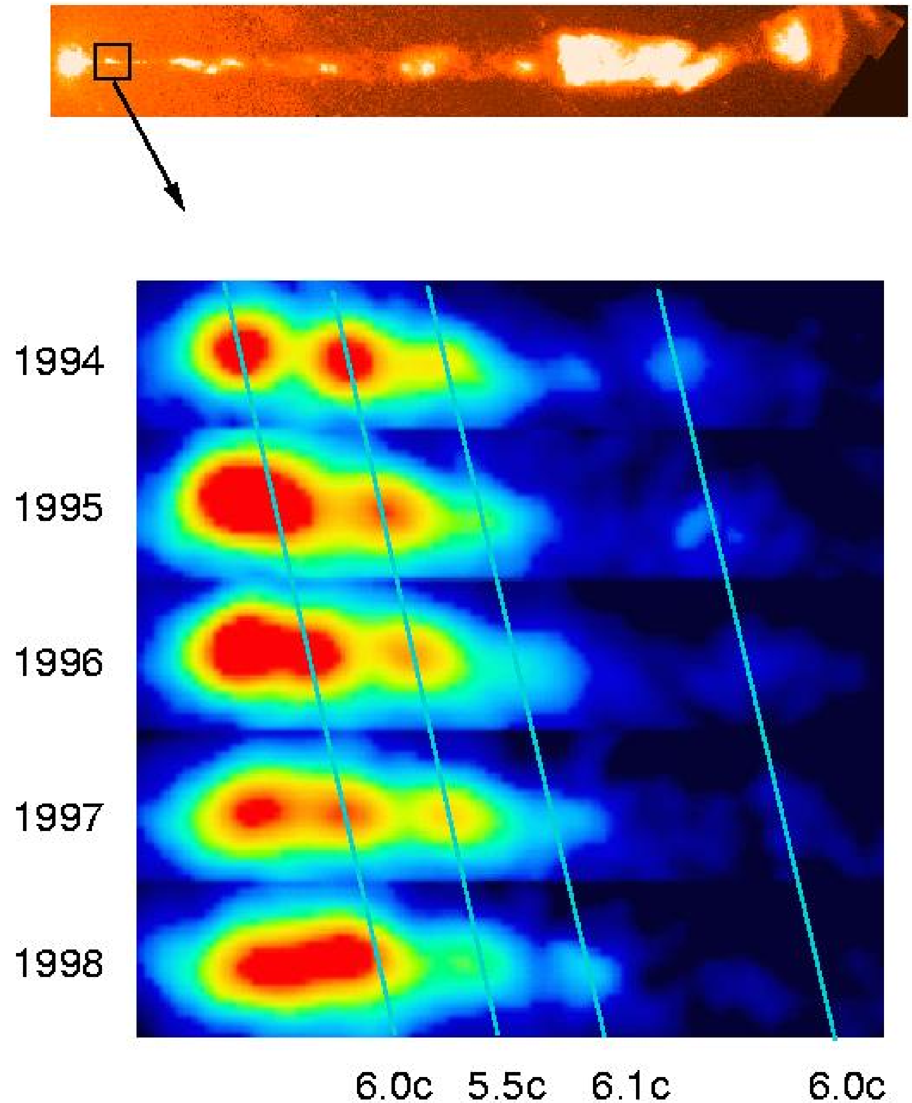

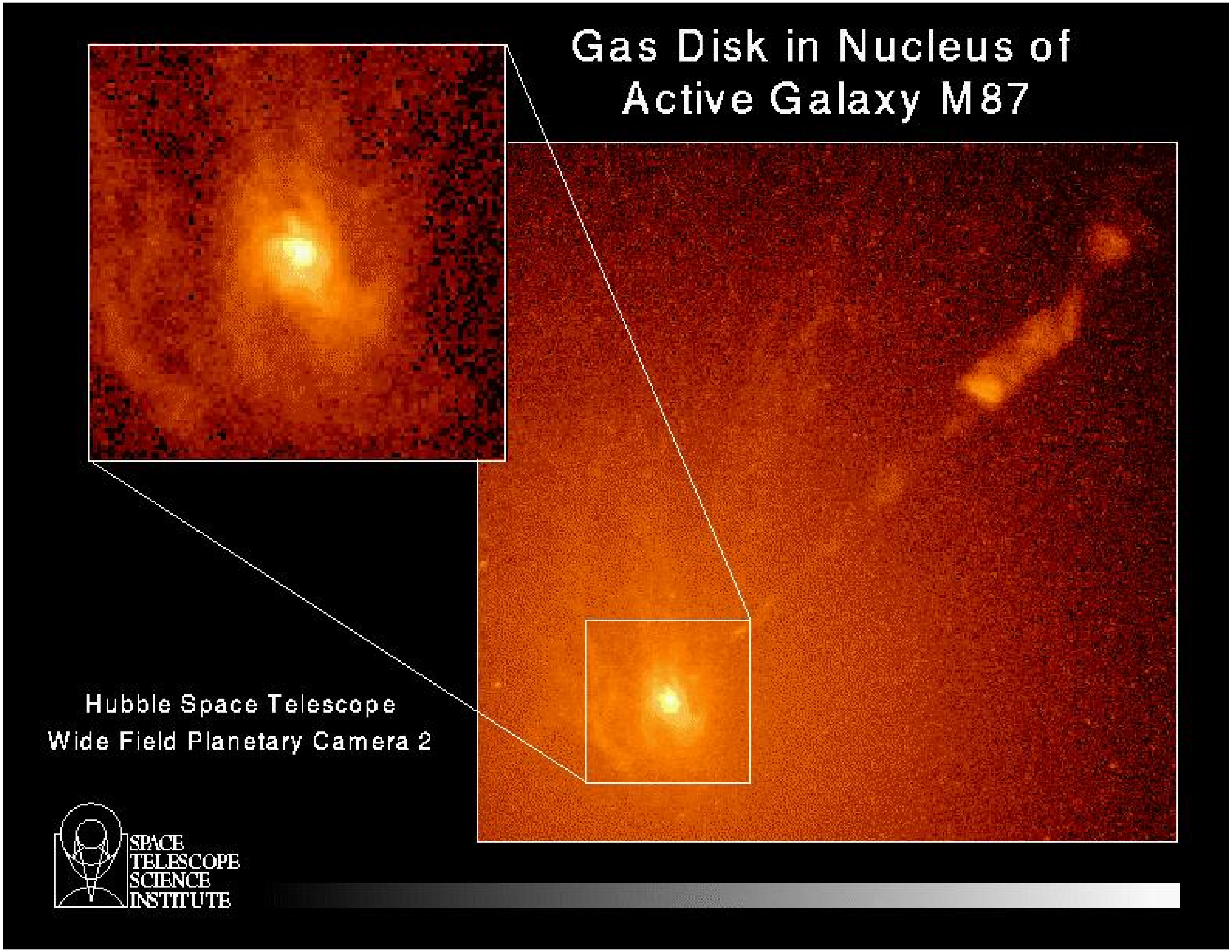
Gas Disk in Nucleus of
Active Galaxy M87
Hubble Space Telescope
Wide Field Planetary Camera 2
SPACE
TELESCOPE
SCIENCE
INSTITUTE

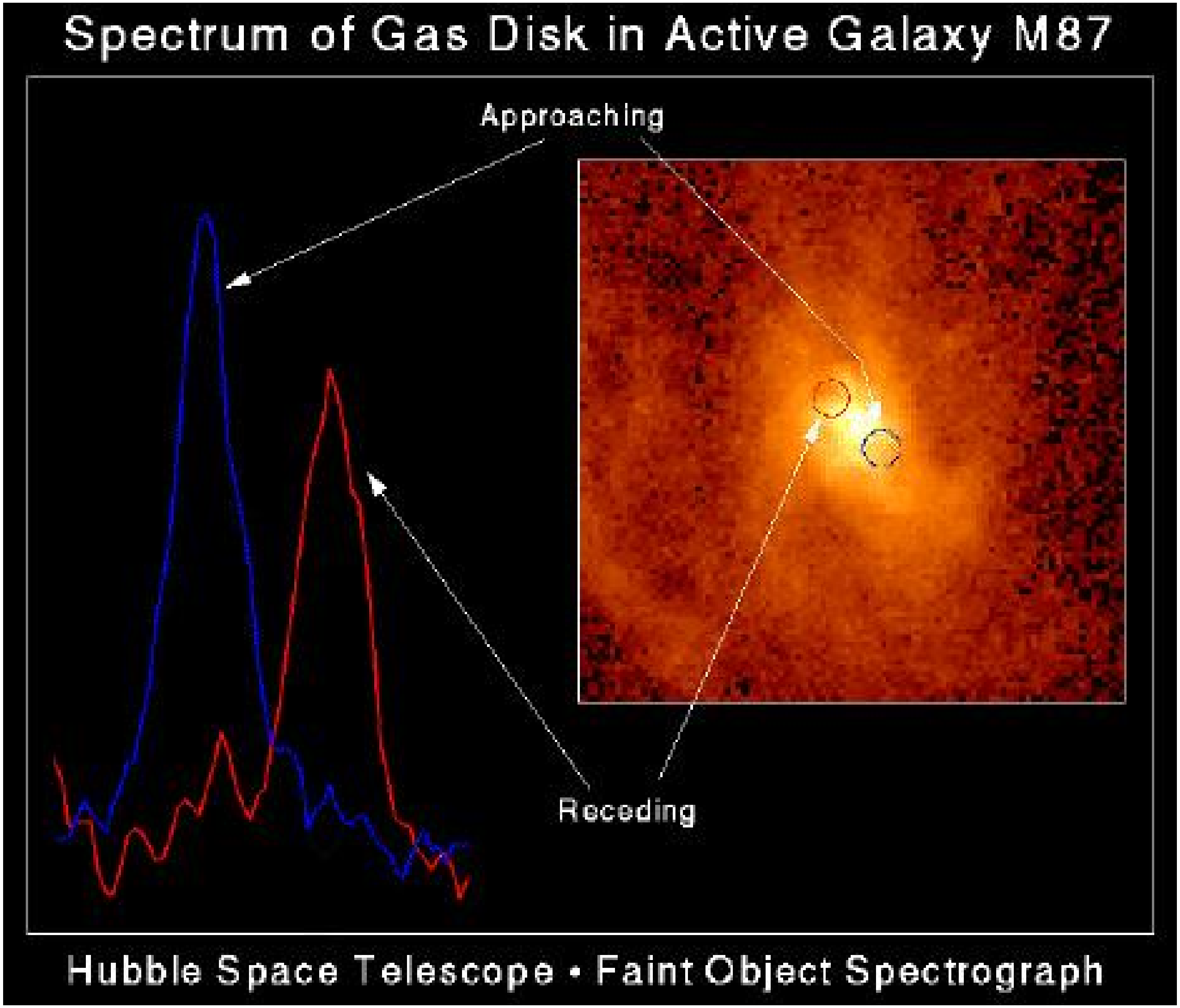
Spectrum of Gas Disk in Active Galaxy M87
Approaching
Receding
Hubble Space Telescope • Faint Object Spectrograph

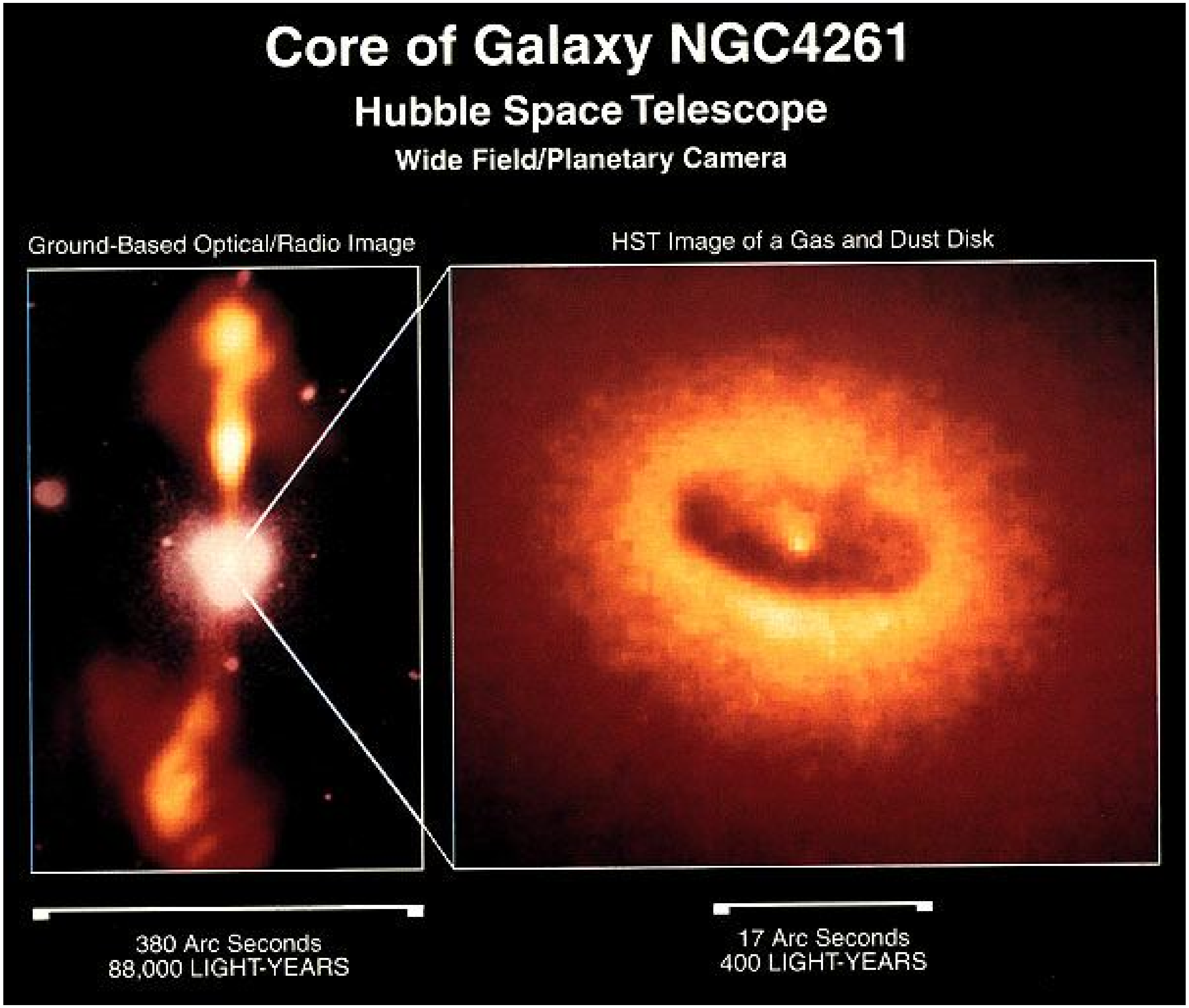

Core of Galaxy NGC4261
Hubble Space Telescope
Wide Field/Planetary Camera
Ground-Based Optical/Radio Image
HST Image of a Gas and Dust Disk
380 Arc Seconds
88,000 LIGHT-YEARS
17 Arc Seconds
400 LIGHT-YEARS

microquasars

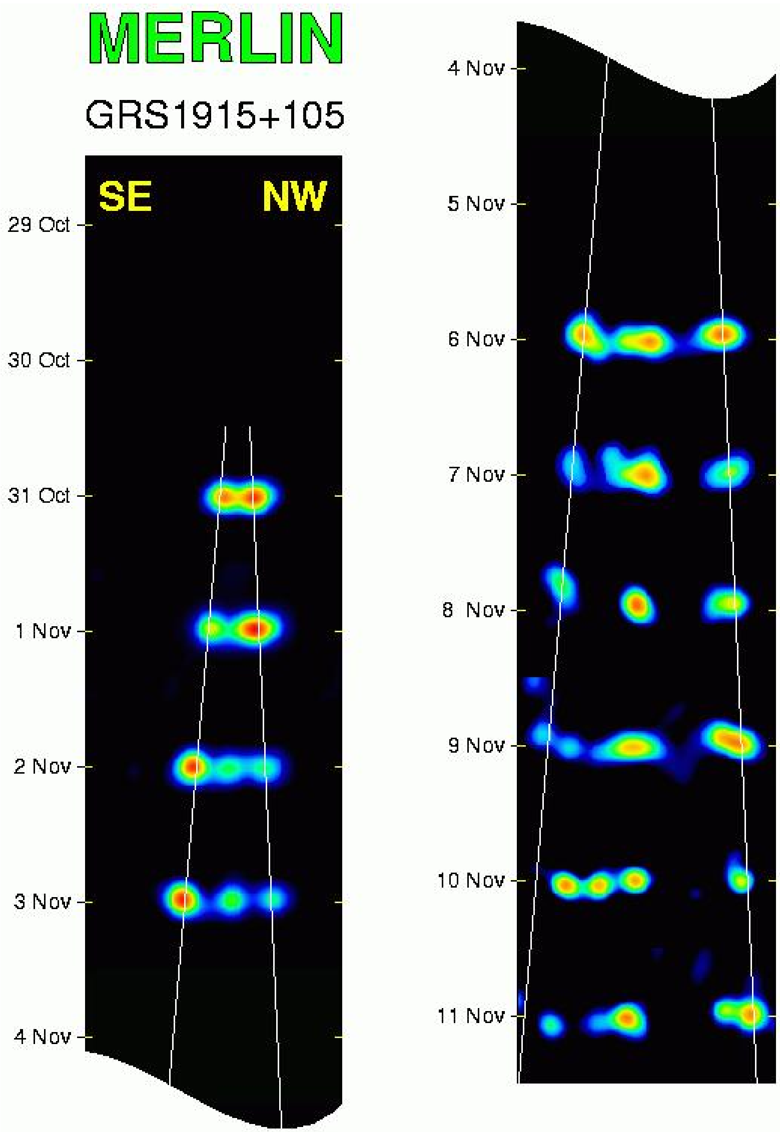

scale-down of quasars

speed $\sim 0.9 - 0.99c$

microquasars

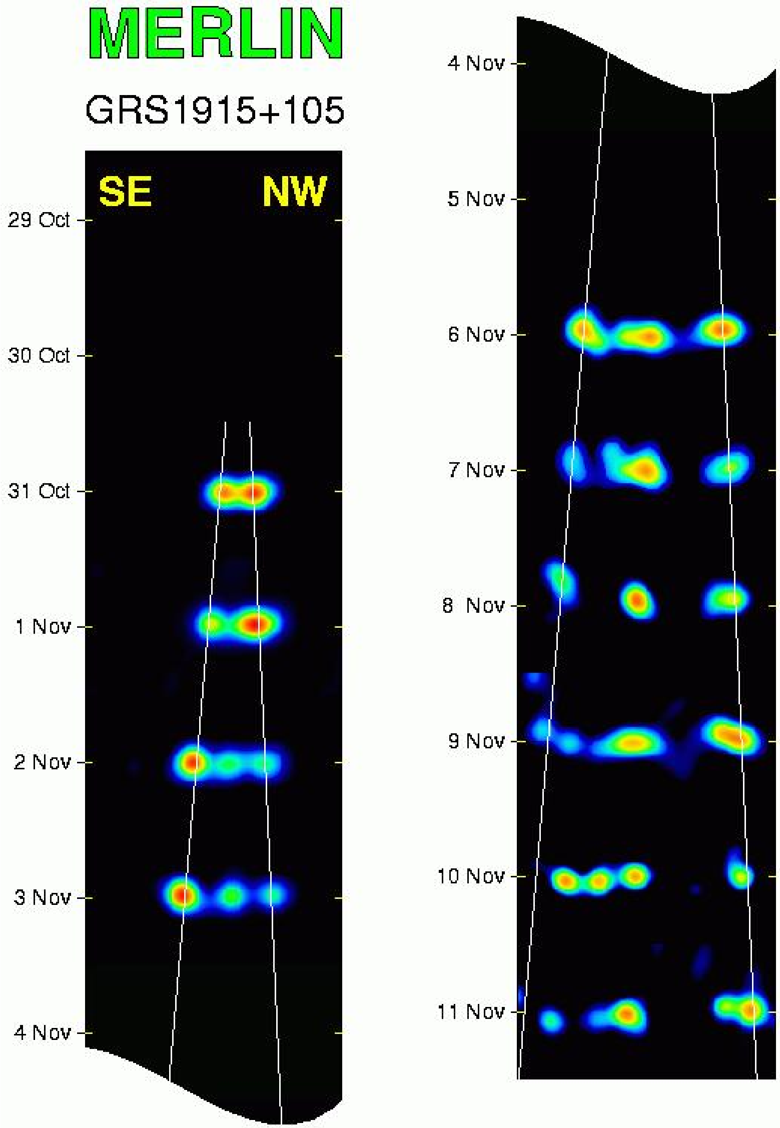

scale-down of quasars

speed $\sim 0.9 - 0.99c$

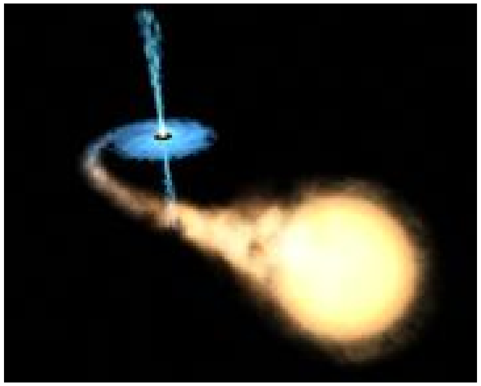

GRBs

- ⋆ high Lorentz factors (compactness problem)
- ⋆ collimated outflows (energy reservoir, achromatic afterglow breaks)

GRBs

- ⋆ high Lorentz factors (compactness problem)
- ⋆ collimated outflows (energy reservoir, achromatic afterglow breaks)

☞ similar characteristics

☞ MHD offers a unified picture

We need magnetic fields

⋆ to extract energy (Poynting flux)

⋆ to extract angular momentum

⋆ to transfer energy and angular momentum to matter

⋆ to explain relatively large-scale acceleration

⋆ to collimate outflows and produce jets

⋆ for synchrotron emission

⋆ to explain polarization maps

MHD (Magneto-Hydro-Dynamic) description

- How the jet is collimated and accelerated? Need to examine outflows taking into account
  - matter: velocity $\boldsymbol{V}$, rest density ρ_0, pressure P, specific enthalpy ξc^2
  - electromagnetic field: $\boldsymbol{E}$, $\boldsymbol{B}$
- ideal MHD equations in special relativity:
  - Maxwell:
    $$\nabla \cdot \boldsymbol{B} = 0 = \nabla \times \boldsymbol{E} + \frac{\partial \boldsymbol{B}}{c \partial t} \, , \; \nabla \times \boldsymbol{B} = \frac{\partial \boldsymbol{E}}{c \partial t} + \frac{4\pi}{c} \boldsymbol{J} \, , \; \nabla \cdot \boldsymbol{E} = \frac{4\pi}{c} J^0$$
  - Ohm: $\boldsymbol{E} + \frac{\boldsymbol{V}}{c} \times \boldsymbol{B} = 0$
  - mass conservation: $\frac{\partial (\gamma \rho_0)}{\partial t} + \nabla \cdot (\gamma \rho_0 \boldsymbol{V}) = 0$
  - specific entropy conservation: $\left(\frac{\partial}{\partial t} + \boldsymbol{V} \cdot \nabla \right) \left(\frac{P}{\rho_0^\Gamma} \right) = 0$
  - momentum: $\gamma \rho_0 \left(\frac{\partial}{\partial t} + \boldsymbol{V} \cdot \nabla \right) (\xi \gamma \boldsymbol{V}) = -\nabla P + \frac{J^0 \boldsymbol{E} + \boldsymbol{J} \times \boldsymbol{B}}{c}$
- The system gives $\boldsymbol{B}$, $\boldsymbol{V}$, ρ_0, P.

Integrals of motion

under the assumption of steady-state and axisymmetry

From $\nabla \cdot \boldsymbol{B} = 0$

$$\boldsymbol{B}_p = \frac{\nabla A \times \hat{\boldsymbol{\phi}}}{\varpi}, \text{ or, } \boldsymbol{B}_p = \nabla \times \left(\frac{A \, \hat{\boldsymbol{\phi}}}{\varpi} \right)$$

$$A = \frac{1}{2\pi} \iint \boldsymbol{B}_p \cdot d\boldsymbol{S}$$

From $\nabla \times \boldsymbol{E} = 0$, $\boldsymbol{E} = -\nabla \Phi$
Because of axisymmetry $E_\phi = 0$.
Combining with Ohm's law
$(\boldsymbol{E} = -\boldsymbol{V} \times \boldsymbol{B}/c)$ we find $\boldsymbol{V}_p \parallel \boldsymbol{B}_p$.

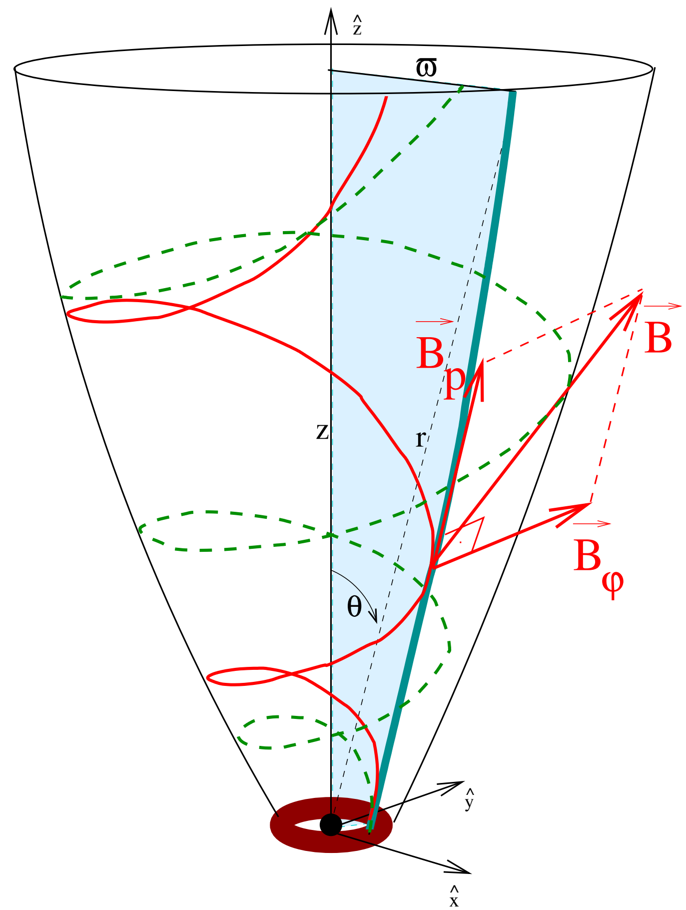

Because $\boldsymbol{V}_p \parallel \boldsymbol{B}_p$ we can write

$$\boldsymbol{V} = \frac{\Psi_A}{4\pi\gamma\rho_0}\boldsymbol{B} + \varpi\Omega\hat{\boldsymbol{\phi}}\,, \quad \frac{\Psi_A}{4\pi\gamma\rho_0} = \frac{V_p}{B_p}\,,$$

$$V_\phi = \frac{\Psi_A}{4\pi\gamma\rho_0}B_\phi + \varpi\Omega = \frac{V_p}{B_p}B_\phi + \varpi\Omega\,.$$

The Ω and Ψ_A are constants of motion, $\Omega = \Omega(A)$, $\Psi_A = \Psi_A(A)$.

- $\Omega =$ angular velocity at the base
- $\Psi_A =$ mass-to-magnetic flux ratio

The electric field $\boldsymbol{E} = -\boldsymbol{V} \times \boldsymbol{B}/c = -(\varpi\Omega/c)\hat{\boldsymbol{\phi}} \times \boldsymbol{B}_p$ is a poloidal vector, normal to $\boldsymbol{B}_p$. Its magnitude is $E = \frac{\varpi\Omega}{c}B_p$.

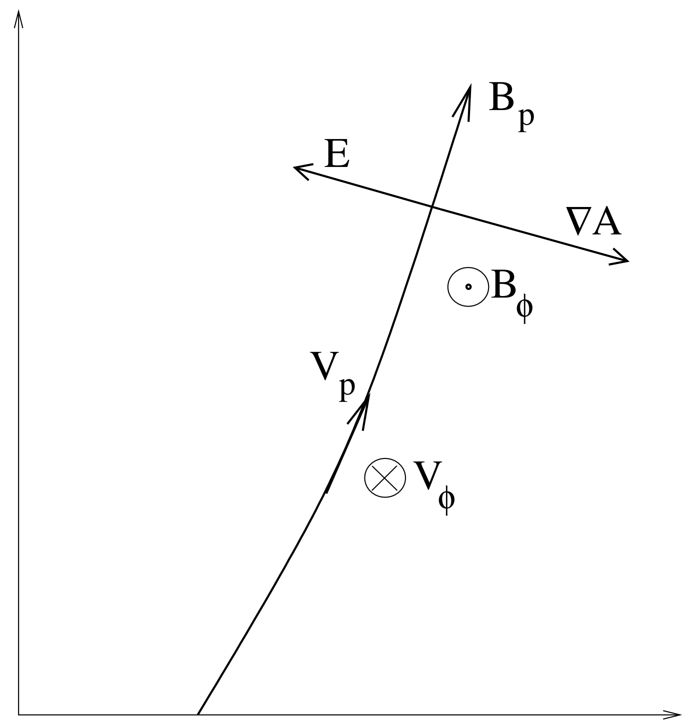

So far, we've used Maxwell's eqs, Ohm's law and the continuity.

The entropy eq gives $P/\rho_0^\Gamma =$ constant of motion (entropy).

We are left with the momentum equation

$$\gamma\rho_0 \left(\boldsymbol{V}\cdot\nabla\right)\left(\xi\gamma\boldsymbol{V}\right) = -\nabla P + \frac{J^0\boldsymbol{E} + \boldsymbol{J}\times\boldsymbol{B}}{c}, \text{ or,}$$

$$\gamma\rho_0 \left(\boldsymbol{V}\cdot\nabla\right)\left(\xi\gamma\boldsymbol{V}\right) = -\nabla P + \frac{(\nabla\cdot\boldsymbol{E})\boldsymbol{E} + (\nabla\times\boldsymbol{B})\times\boldsymbol{B}}{4\pi}$$

Due to axisymmetry, the toroidal component can be integrated to give the total angular momentum-to-mass flux ratio:

$$\xi\gamma\varpi V_\phi - \frac{\varpi B_\phi}{\Psi_A} = L(A)$$

Poloidal components of the momentum eq

$$\gamma\rho_0 \left(\boldsymbol{V}\cdot\nabla\right)\left(\xi\gamma\boldsymbol{V}\right) = -\nabla P + \frac{(\nabla\cdot\boldsymbol{E})\boldsymbol{E} + (\nabla\times\boldsymbol{B})\times\boldsymbol{B}}{4\pi} \Leftrightarrow$$

$$\boldsymbol{f}_G + \boldsymbol{f}_T + \boldsymbol{f}_C + \boldsymbol{f}_I + \boldsymbol{f}_P + \boldsymbol{f}_E + \boldsymbol{f}_B = 0$$

$$\left.\begin{array}{lll} \boldsymbol{f}_G = -\gamma\rho_0\xi\left(\boldsymbol{V}\cdot\nabla\gamma\right)\boldsymbol{V} & & \\ \boldsymbol{f}_T = -\gamma^2\rho_0\left(\boldsymbol{V}\cdot\nabla\xi\right)\boldsymbol{V} & : & \text{“temperature” force} \\ \boldsymbol{f}_C = \hat{\boldsymbol{\varpi}}\gamma^2\rho_0\xi V_\phi^2/\varpi & : & \text{centrifugal force} \\ \boldsymbol{f}_I = -\gamma^2\rho_0\xi\left(\boldsymbol{V}\cdot\nabla\right)\boldsymbol{V} - \boldsymbol{f}_C & & \end{array}\right\} \text{inertial force}$$

$$\begin{array}{lll} \boldsymbol{f}_P = -\nabla P & : & \text{pressure force} \\ \boldsymbol{f}_E = \left(\nabla\cdot\boldsymbol{E}\right)\boldsymbol{E}/4\pi & : & \text{electric force} \\ \boldsymbol{f}_B = \left(\nabla\times\boldsymbol{B}\right)\times\boldsymbol{B}/4\pi & : & \text{magnetic force} \end{array}$$

Acceleration mechanisms

- thermal (due to ∇P) $\rightarrow$ velocities up to C_s
- magnetocentrifugal (beads on wire - Blandford & Payne)
  - initial half-opening angle $\vartheta > 30^o$
  - the $\vartheta > 30^o$ not necessary for nonnegligible P
  - velocities up to $\varpi_0 \Omega$
- relativistic thermal (thermal fireball) gives $\gamma \sim \xi_i$, where $\xi = \dfrac{\text{enthalpy}}{\text{mass} \times c^2}$.
- magnetic

All acceleration mechanisms can be seen in the energry conservation equation

$$\mu = \xi\gamma + \frac{\Omega}{\Psi_A c^2}\varpi|B_\phi| \left(\text{where } \mu = \frac{\frac{dE}{dSdt}}{\frac{dM}{dSdt}c^2} \right)$$

So $\gamma \uparrow$ when $\xi \downarrow$ (thermal, relativistic thermal), or, $\varpi|B_\phi| \downarrow \Leftrightarrow I_p \downarrow$ (magnetocentrifugal, magnetic).

The efficiency of the magnetic acceleration

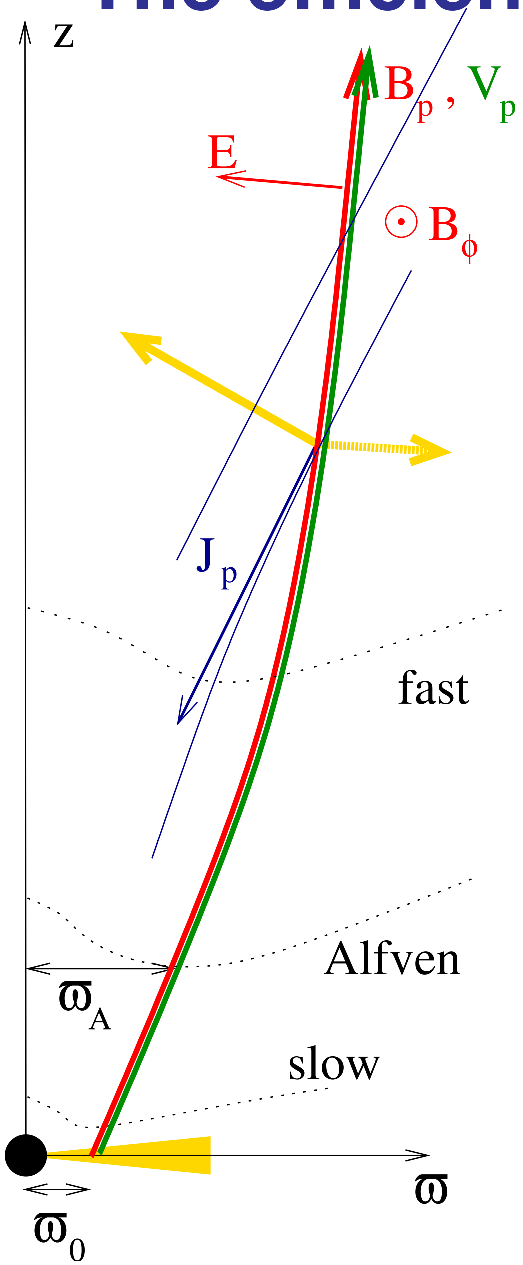

The $\boldsymbol{J}_p \times \boldsymbol{B}_\phi$ force strongly depends on the angle between field-lines and current-lines (loci of $\varpi B_\phi =$ const).

These two families of lines are connected:

From Ferraro's law, $V_\phi = \frac{V_p}{B_p} B_\phi + \varpi \Omega \rightarrow$ $\varpi |B_\phi| \approx \varpi^2 B_p \Omega / V_p$.

The transfield force-balance determines the acceleration.

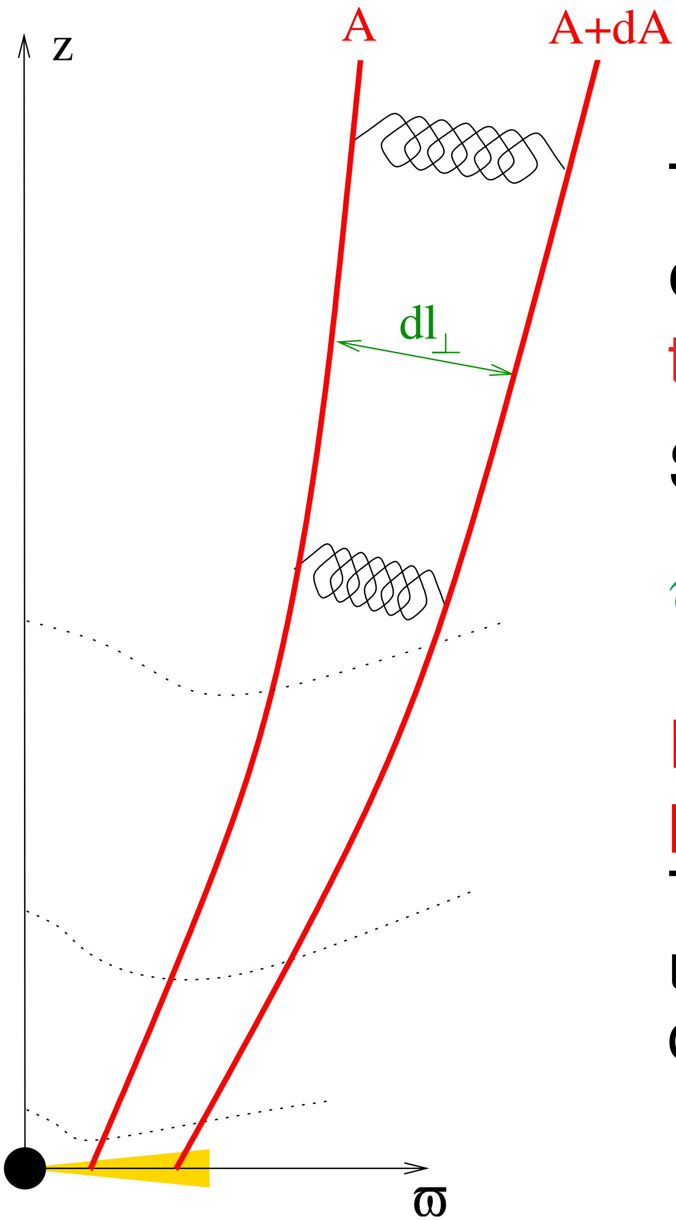

The magnetic field minimizes its energy under the condition of keeping the magnetic flux constant.

So, $\varpi|B_\phi| \downarrow$ for decreasing

$$\varpi^2 B_p = \frac{\varpi^2}{2\pi\varpi dl_\perp}(\underbrace{B_p dS}_{dA}) \propto \frac{\varpi}{dl_\perp}.$$

Expansion with increasing $dl_\perp/\varpi$ leads to acceleration (Vlahakis 2004). The expansion ends in a more-or-less uniform distribution $\varpi^2 B_p \approx A$ (in a quasi-monopolar shape).

Conclusions on the magnetic acceleration

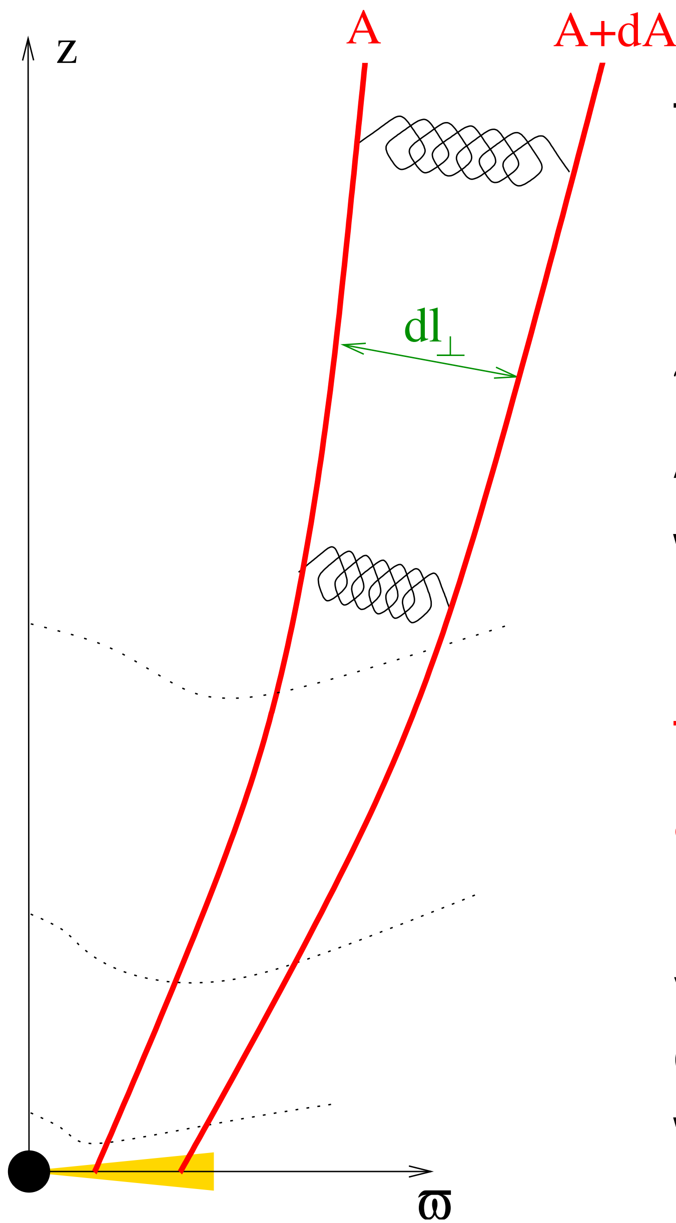

If we start with a uniform distribution the magnetic energy is already minimum $\rightarrow$ no acceleration. Example: Michel's (1969) solution which gives $\gamma_\infty \approx \mu^{1/3} \ll \mu$.

Also Beskin et al (1998); Bogovalov (2001) who found quasi-monopolar solutions.

For any other (more realistic) initial field distribution we have efficient acceleration!

(details and an analytical estimation of the efficiency in Vlahakis 2004, ApSS 293, 67).

example: if we start with $\varpi^2 B_p / A = 2$ we have asymptotically $\varpi^2 B_p / A = 1$ $\rightarrow 50\%$ efficiency

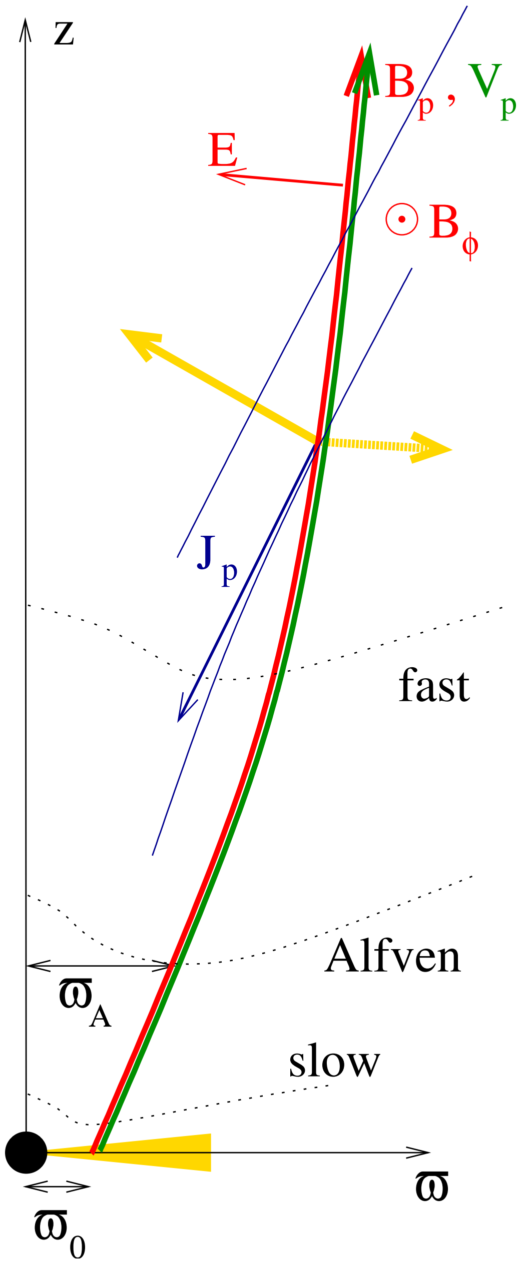

On the collimation

The $\boldsymbol{J}_p \times \boldsymbol{B}_\phi$ force contributes to the collimation (hoop-stress).
In relativistic flows the electric force plays an opposite role (a manifestation of the high inertia of the flow).

- collimation by an external wind (Bogovalov & Tsinganos 2005, for AGN jets)
- surrounding medium may play a role (in the collapsar model)
- self-collimation mainly works at small distances where the velocities are mildly relativistic (Vlahakis & Königl 2003)

For $\gamma \gg 1$, the transfield force-balance gives

$$\gamma^2 \frac{\varpi}{\mathcal{R}} \approx \underbrace{\left(1 - \frac{\gamma}{\mu}\right) \varpi \nabla \ln \left| \frac{\Psi_A}{\Omega} \left(\frac{\mu}{\gamma} - 1\right) \right| \cdot \frac{\nabla A}{|\nabla A|}}_{\mathcal{O}(1)} - \left(\frac{\gamma}{\varpi \Omega / c}\right)^2 \underbrace{\frac{\hat{\varpi} \cdot \nabla A}{|\nabla A|}}_{\mathcal{O}(1)}$$

- If the last term is negligible then the curvature radius $\mathcal{R} \sim \gamma^2 \varpi$ ($\gg \varpi$).

Collimation more difficult, but not impossible!

$$\frac{\varpi}{\mathcal{R}} = -\varpi \frac{\partial^2 \varpi}{\partial z^2} \left(\frac{B_z}{B_p}\right)^3 \sim \left(\frac{\varpi}{z}\right)^2$$

Combining the above, we get

$$\gamma \sim \frac{z}{\varpi} \qquad \text{– same from } (t =) \; \frac{z}{V_z} = \frac{\varpi}{V_\varpi} \Leftrightarrow \frac{z}{c} = \frac{\varpi}{\sqrt{c^2 - V_z^2}} \approx \frac{\varpi}{c/\gamma}$$

- If the first term is negligible (quasi-radial flow) then

$$\gamma \approx \varpi \Omega / c$$

(linear accelerator, Contopoulos & Kazanas 2002)

r self-similarity

Assume that all physical quantities (velocity and magnetic field components, pressure, density) scale as a power of r times a function of θ (in spherical coordinates).

$$B_r = r^{F-2}\mathcal{C}_1(\theta)\,,\; B_\phi = r^{F-2}\mathcal{C}_2(\theta)\,,$$
$$V_r/c = \mathcal{C}_3(\theta)\,,\; V_\theta/c = -\mathcal{C}_4(\theta)\,,\; V_\phi/c = \mathcal{C}_5(\theta)\,,$$
$$\rho_0 = r^{2(F-2)}\mathcal{C}_6(\theta)\,,\; P = r^{2(F-2)}\mathcal{C}_7(\theta)\,.$$

The variables $r\,,\theta$ are separable and the system reduces to ODEs.

- Blandford & Payne – (nonrelativistic)
- Li, Chiueh, & Begelman (1992) and Contopoulos (1994) – (cold)
- Vlahakis & Königl (2003, 2004) – (including thermal/radiation effects)

Semi-analytic solutions for GRB Jets (NV & Königl 2001, 2003a,b)

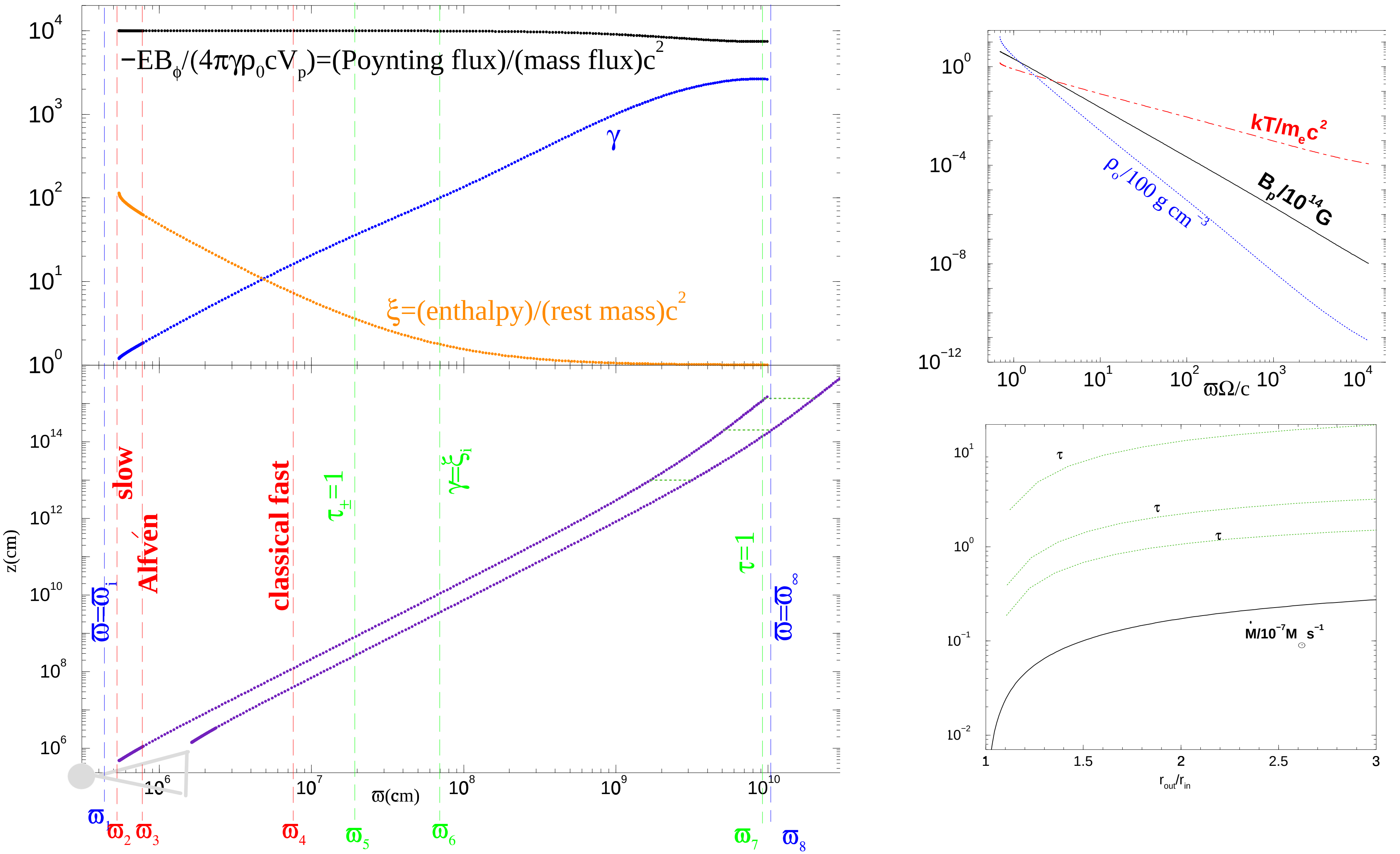

- $\varpi_1 < \varpi < \varpi_6$: Thermal acceleration - force free magnetic field ($\gamma \propto \varpi$, $\rho_0 \propto \varpi^{-3}$, $T \propto \varpi^{-1}$, $\varpi B_\phi = const$, parabolic shape of fieldlines: $z \propto \varpi^2$)
- $\varpi_6 < \varpi < \varpi_8$: Magnetic acceleration ($\gamma \propto \varpi$, $\rho_0 \propto \varpi^{-3}$)
- $\varpi = \varpi_8$: cylindrical regime - equipartition $\gamma_\infty \approx (-EB_\phi/4\pi\gamma\rho_0 V_p)_\infty$

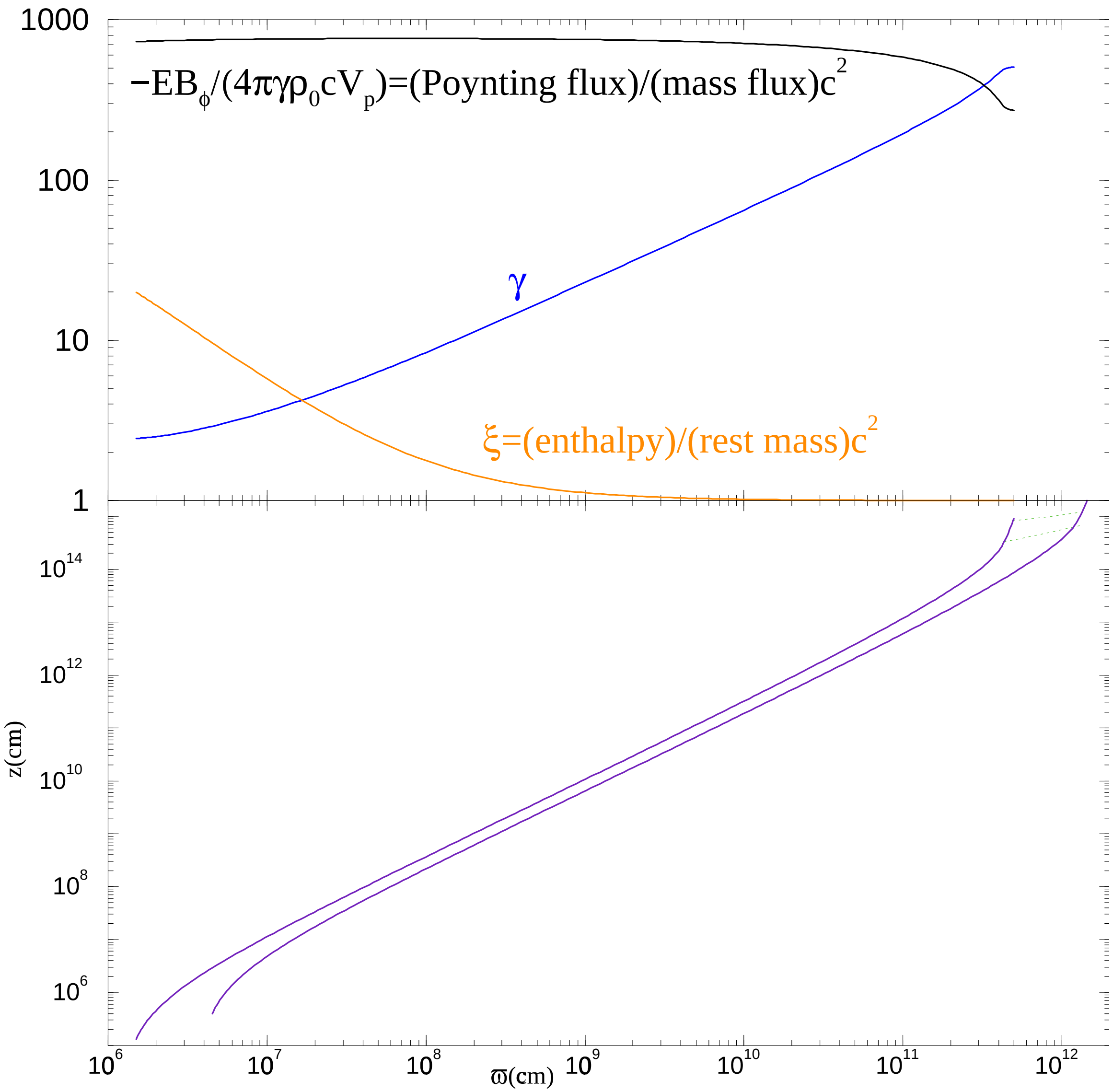

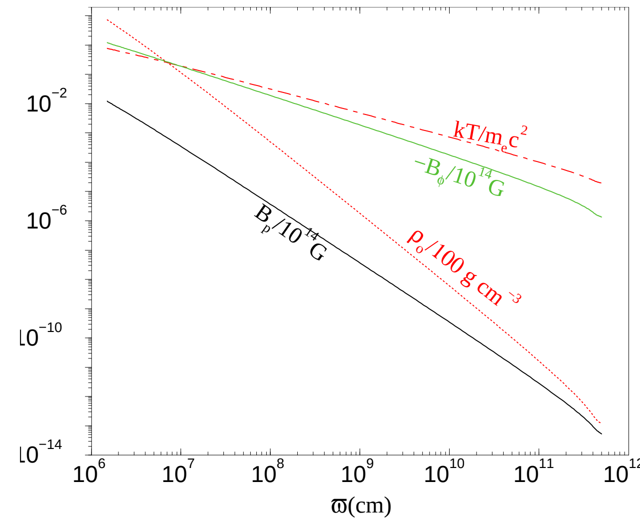

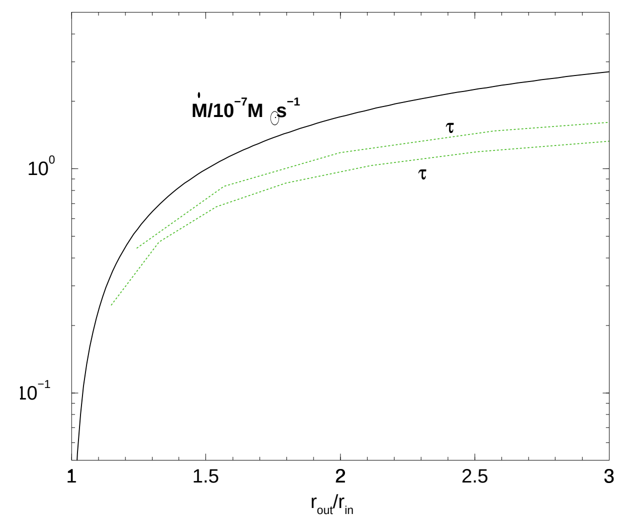

- Thermal acceleration ($\gamma \propto \varpi^{0.44}$, $\rho_0 \propto \varpi^{-2.4}$, $T \propto \varpi^{-0.8}$, $B_\phi \propto \varpi^{-1}$, $z \propto \varpi^{1.5}$)
- Magnetic acceleration ($\gamma \propto \varpi^{0.44}$, $\rho_0 \propto \varpi^{-2.4}$)
- cylindrical regime - equipartition $\gamma_\infty \approx (-EB_\phi/4\pi\gamma\rho_0 V_p)_\infty$

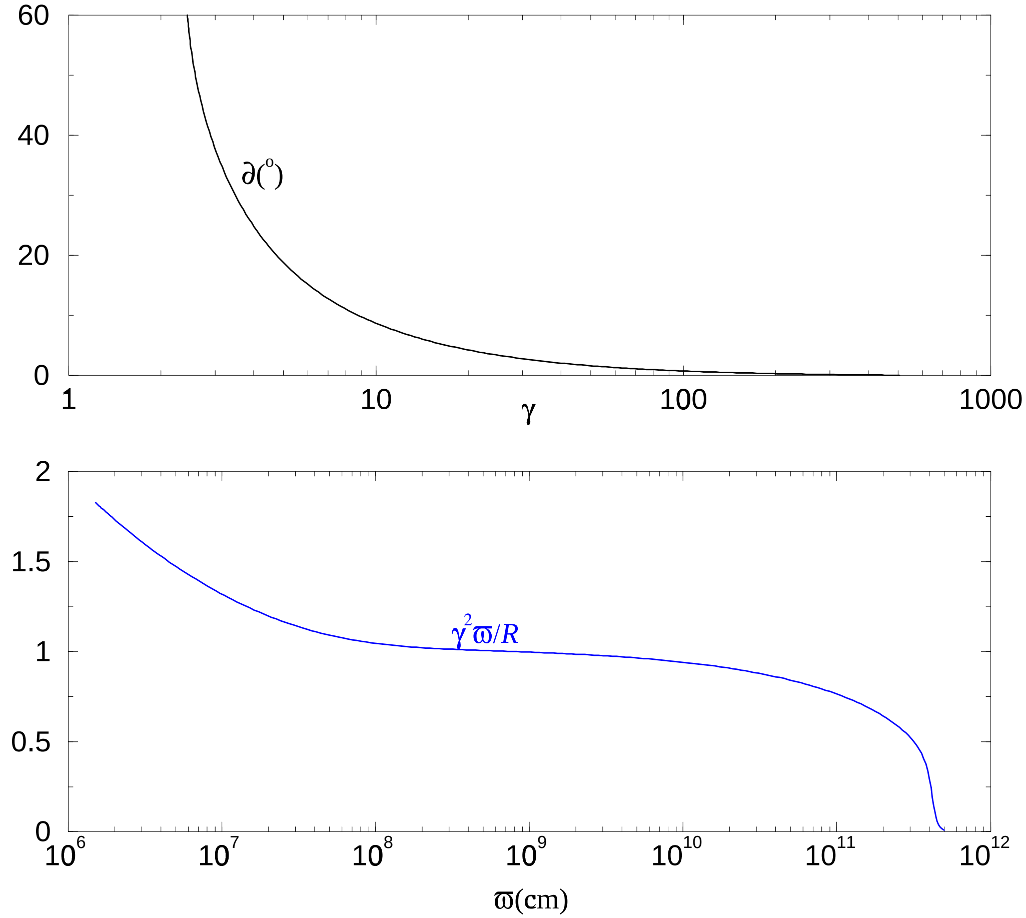

- $\star$ At $\varpi = 10^8$cm – where $\gamma = 10$ – the opening half-angle is already $\vartheta = 10^o$
- $\star$ For $\varpi > 10^8$cm, collimation continues slowly ($\mathcal{R} \sim \gamma^2\varpi$)

Semi-analytic solutions for AGN jets (Vlahakis & Königl 2004)

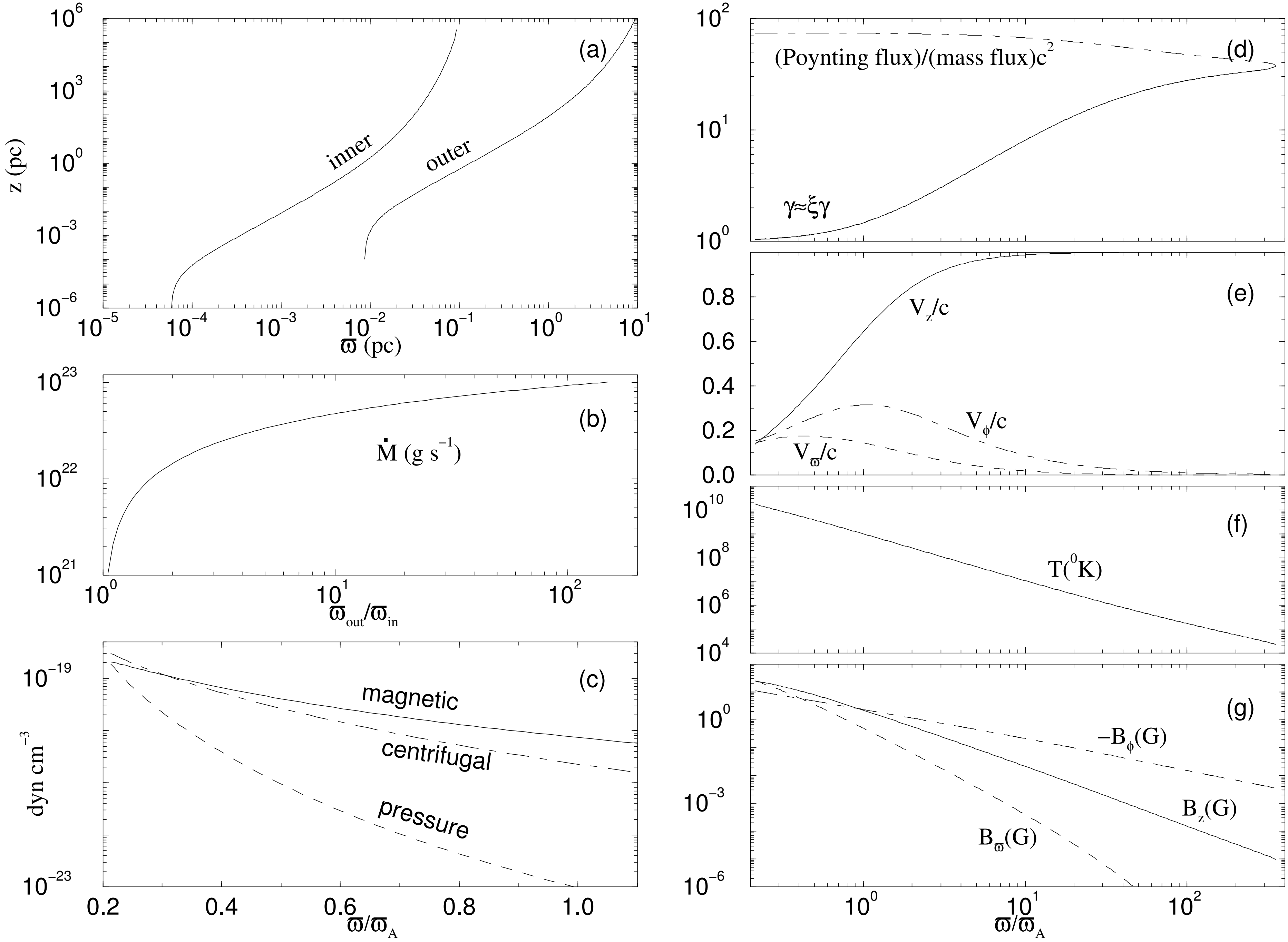

Simulations of relativistic AGN jets

Komissarov, Barkov, Vlahakis, & Königl (2007)

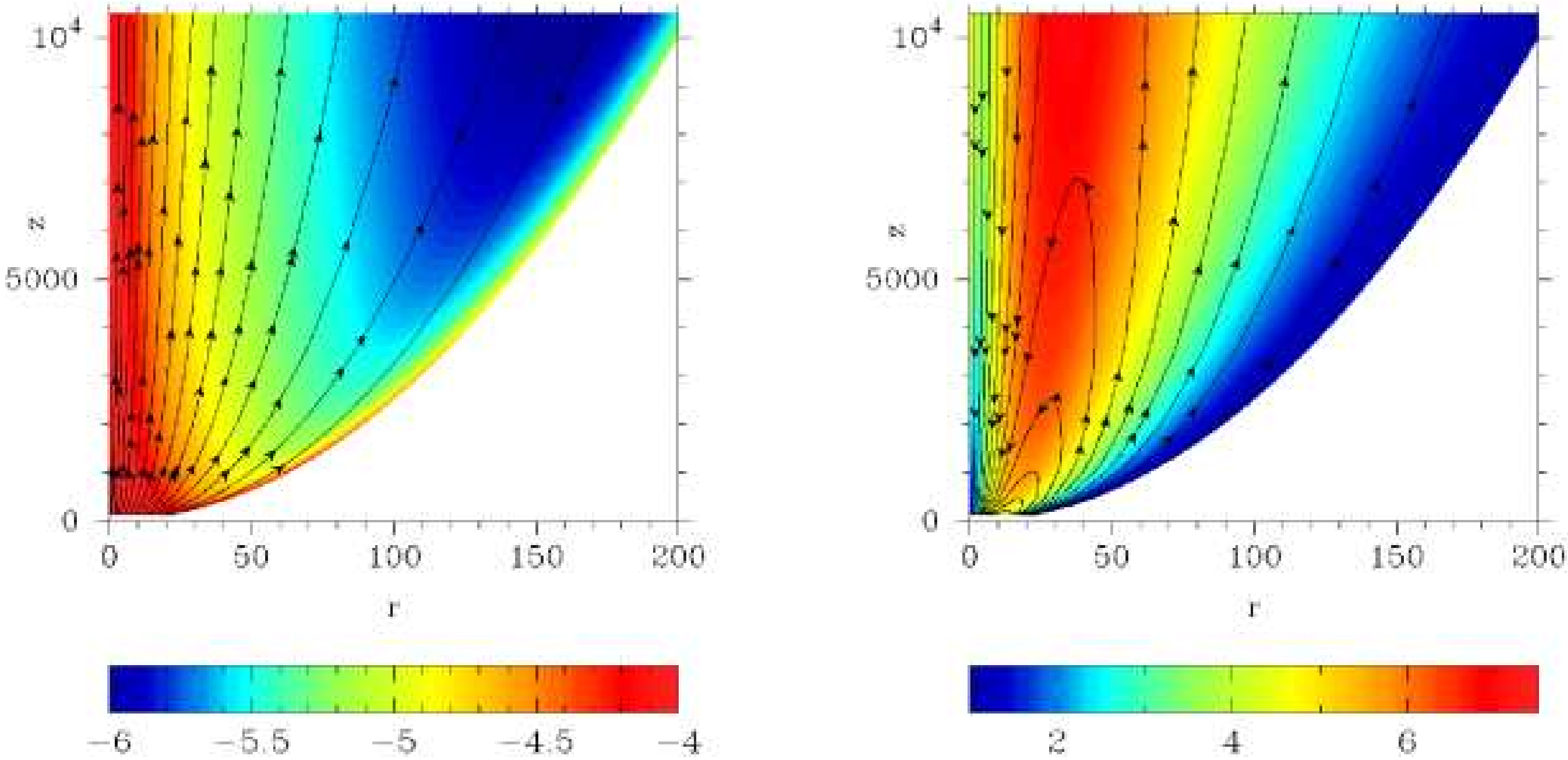

Left panel shows density (colour) and magnetic field lines.
Right panel shows the Lorentz factor (colour) and the current lines.

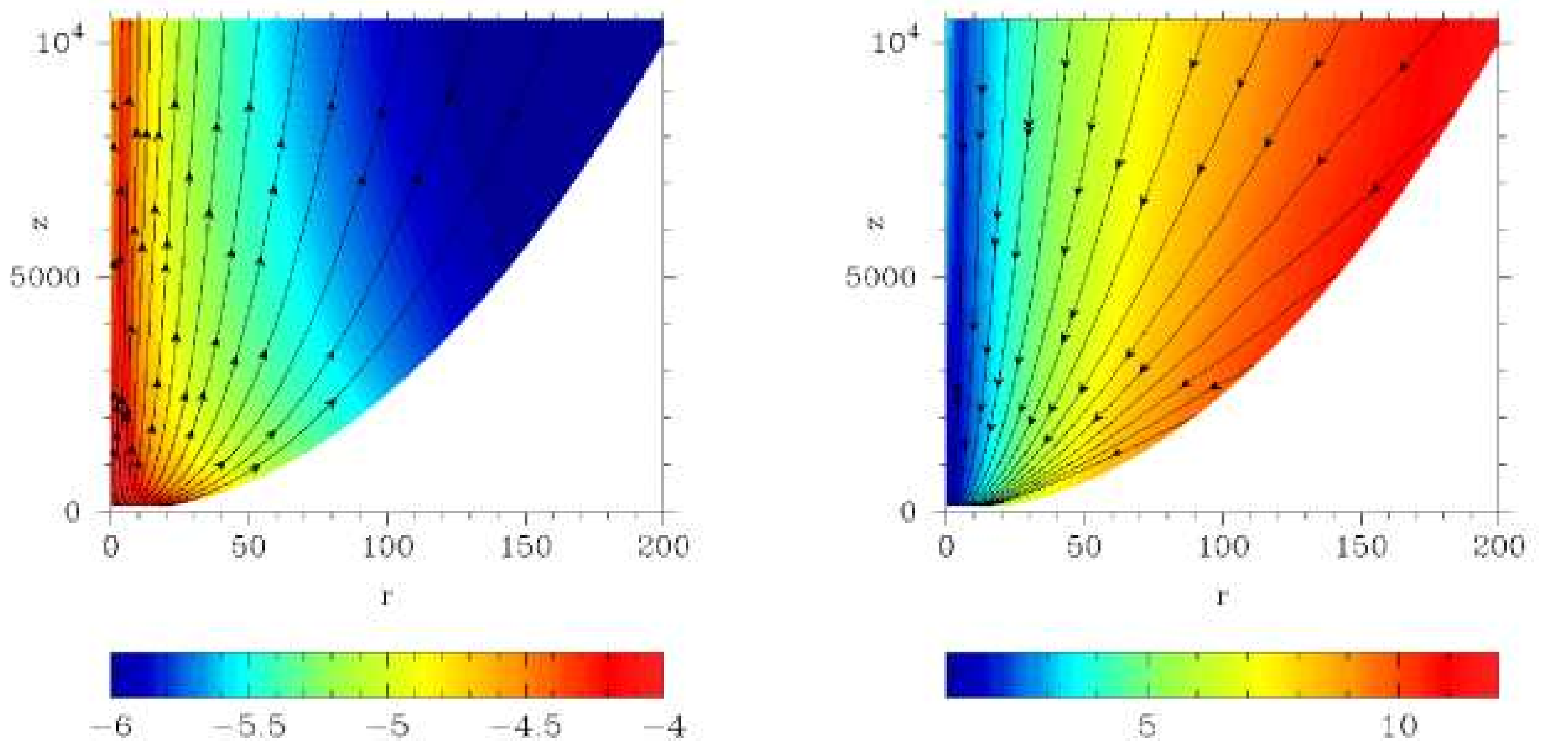

10^4
z
5000
0
0
50
100
150
200
r
−6
−5.5
−5
−4.5
−4
5
10

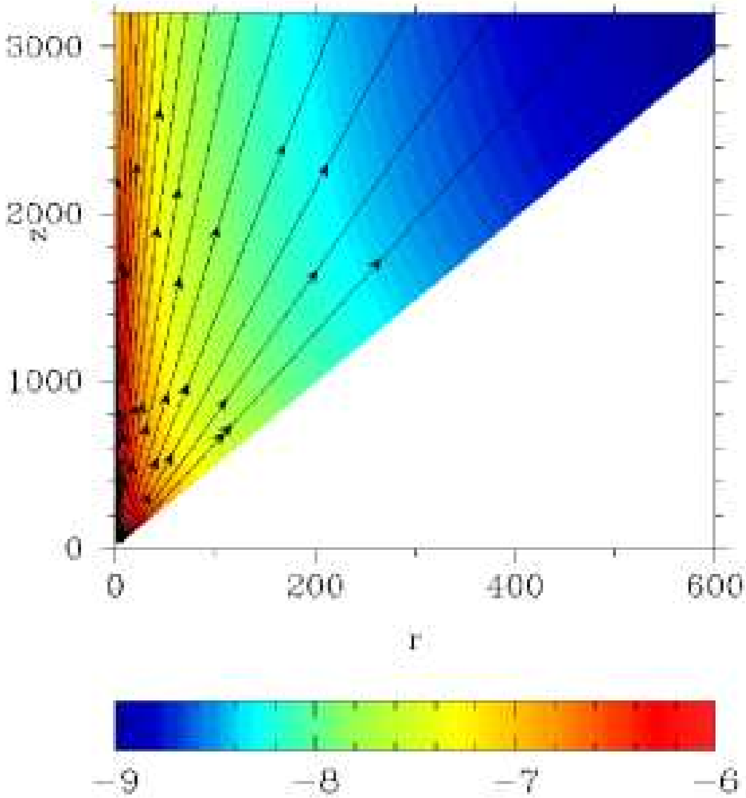
3000
2000
z
1000
0
0
200
400
600
r
−9
−8
−7
−6

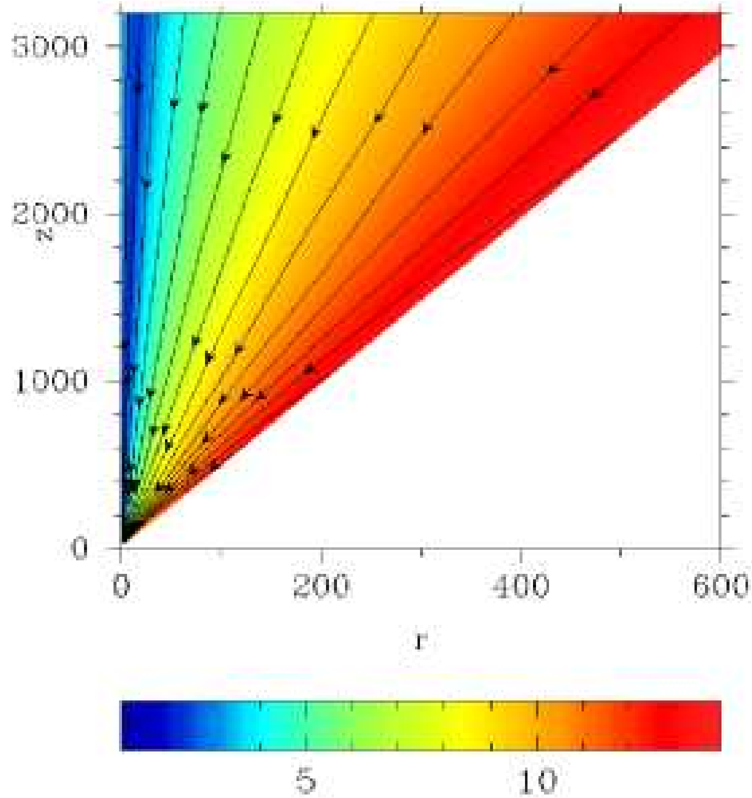
3000
2000
z
1000
0
0
200
400
600
r
5
10

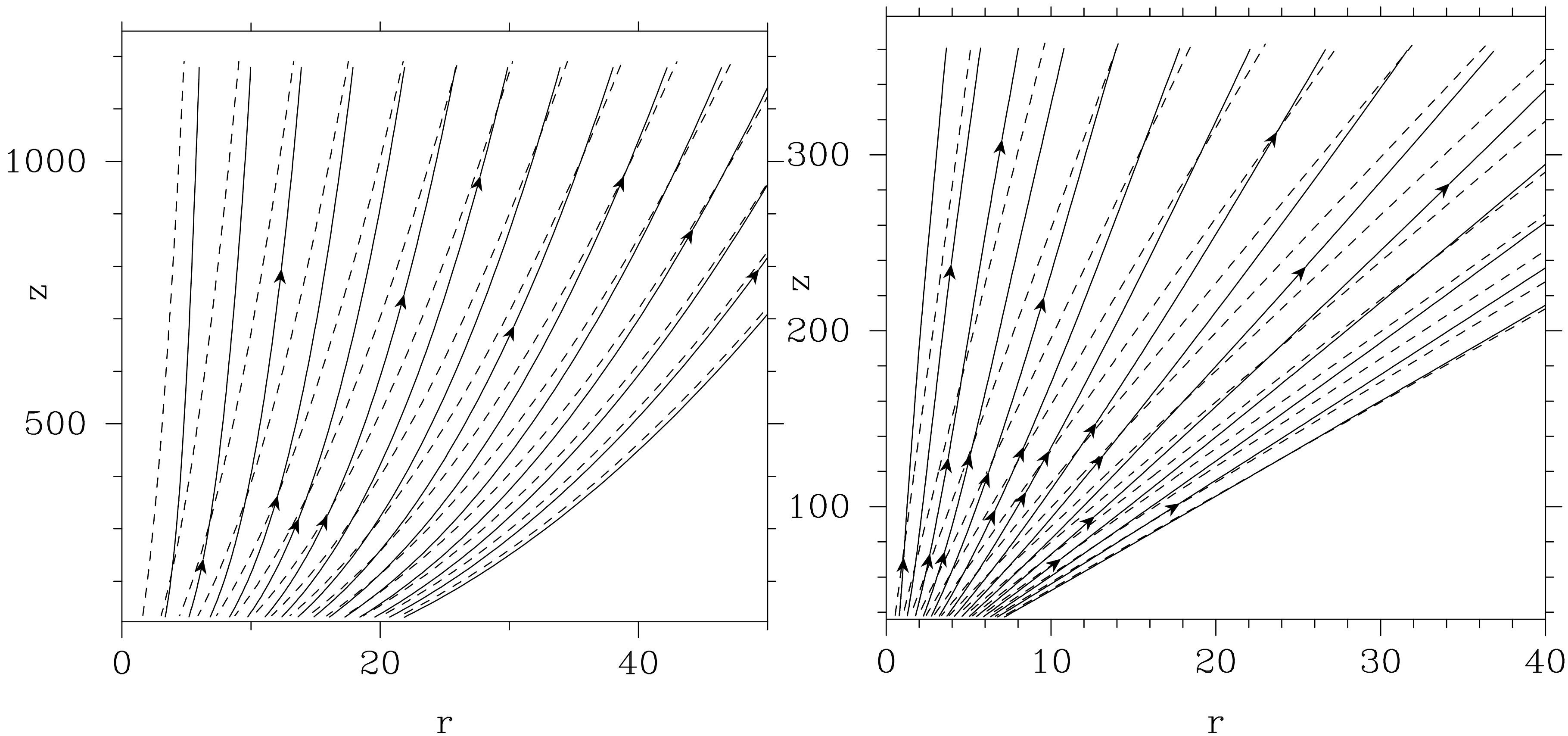
1000
500
z
0
20
40
r
300
200
100
z
0
10
20
30
40
r

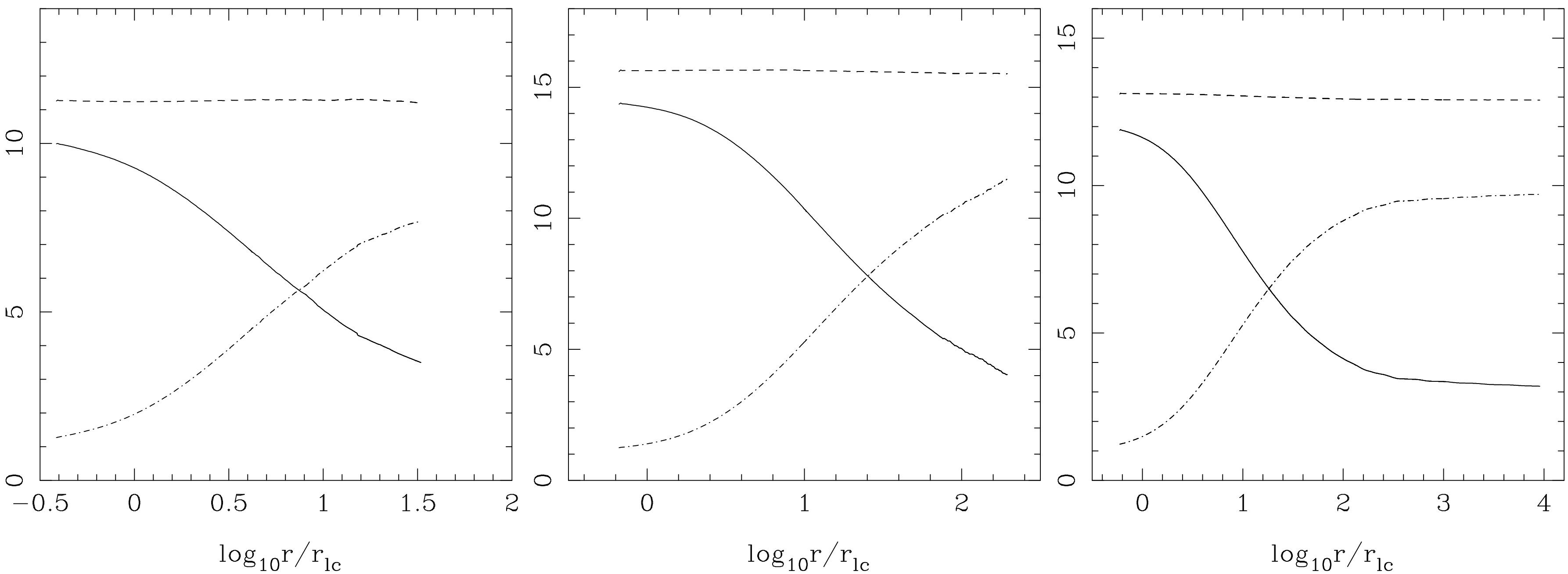

$\gamma\sigma$ (solid line), μ (dashed line) and γ (dash-dotted line) along a magnetic field line as a function of cylindrical radius for models C1 (left panel), C2 (middle panel) and A2 (right panel).

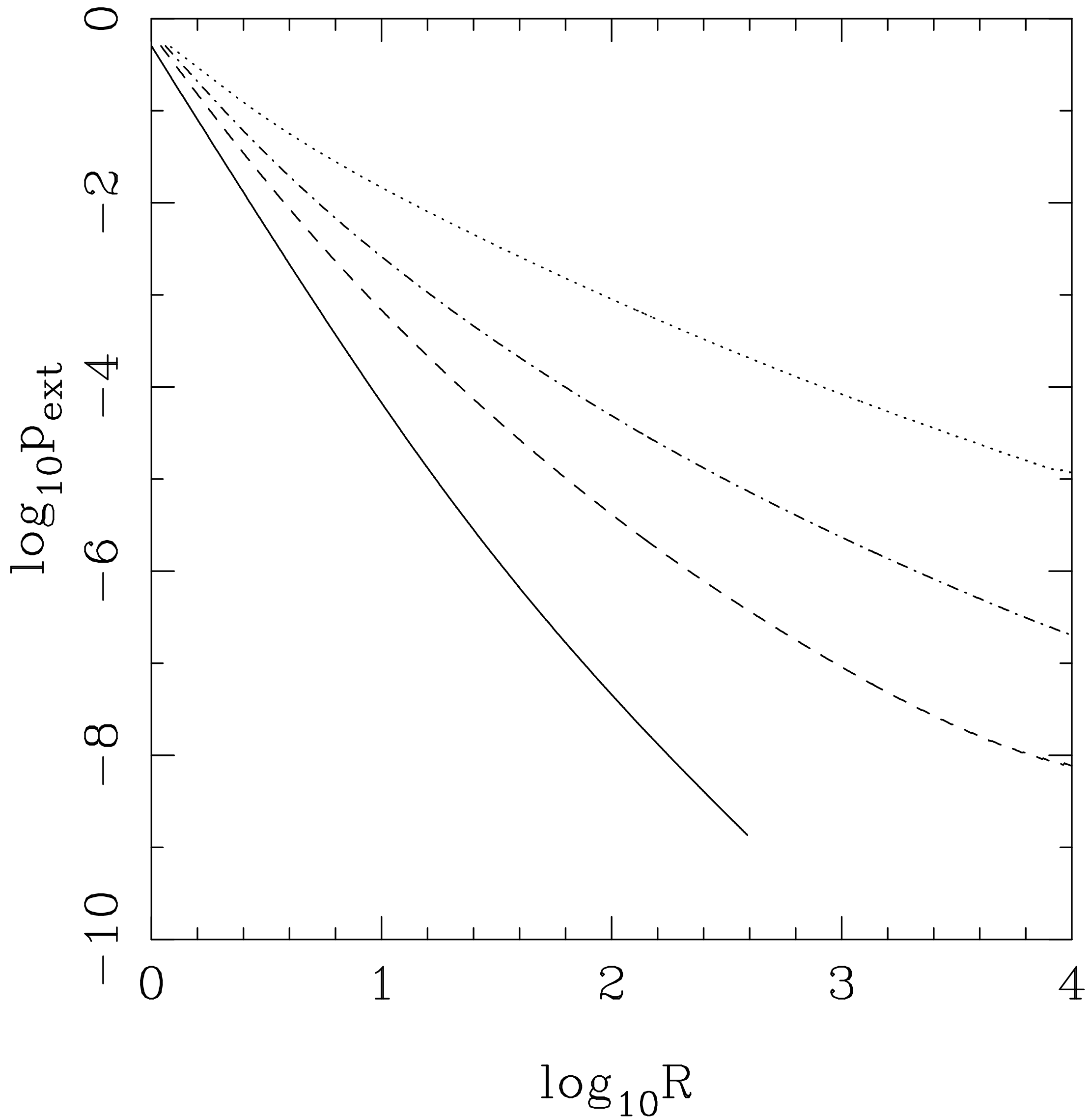

external pressure $P_{ext} = (B^2 - E^2)/8\pi$

(without a wall)

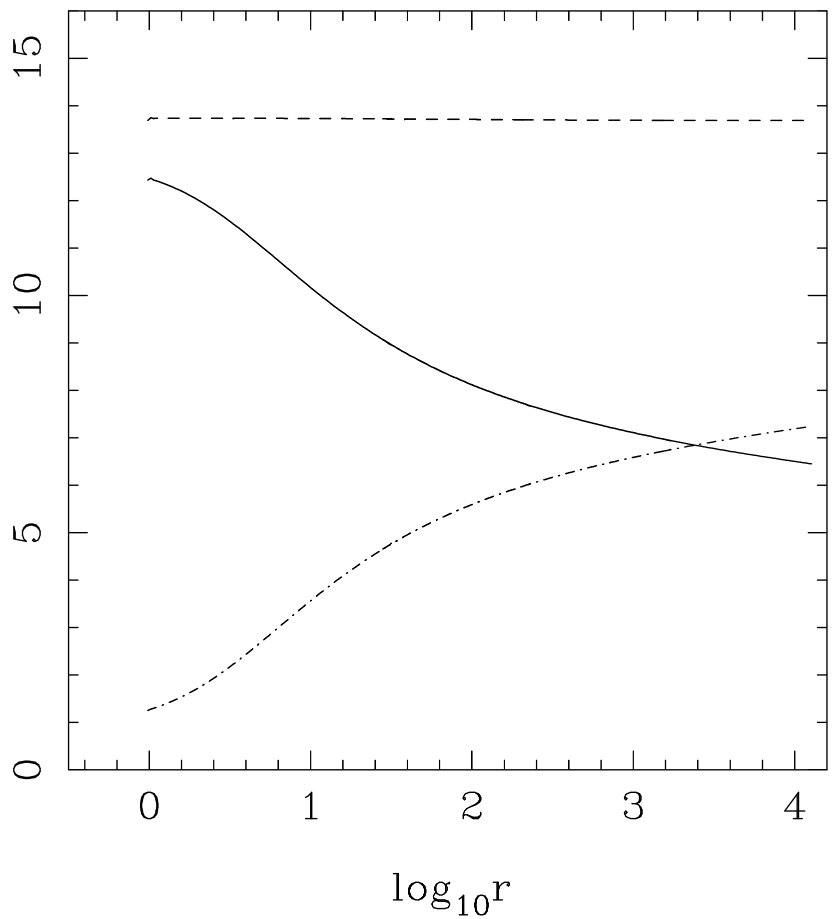

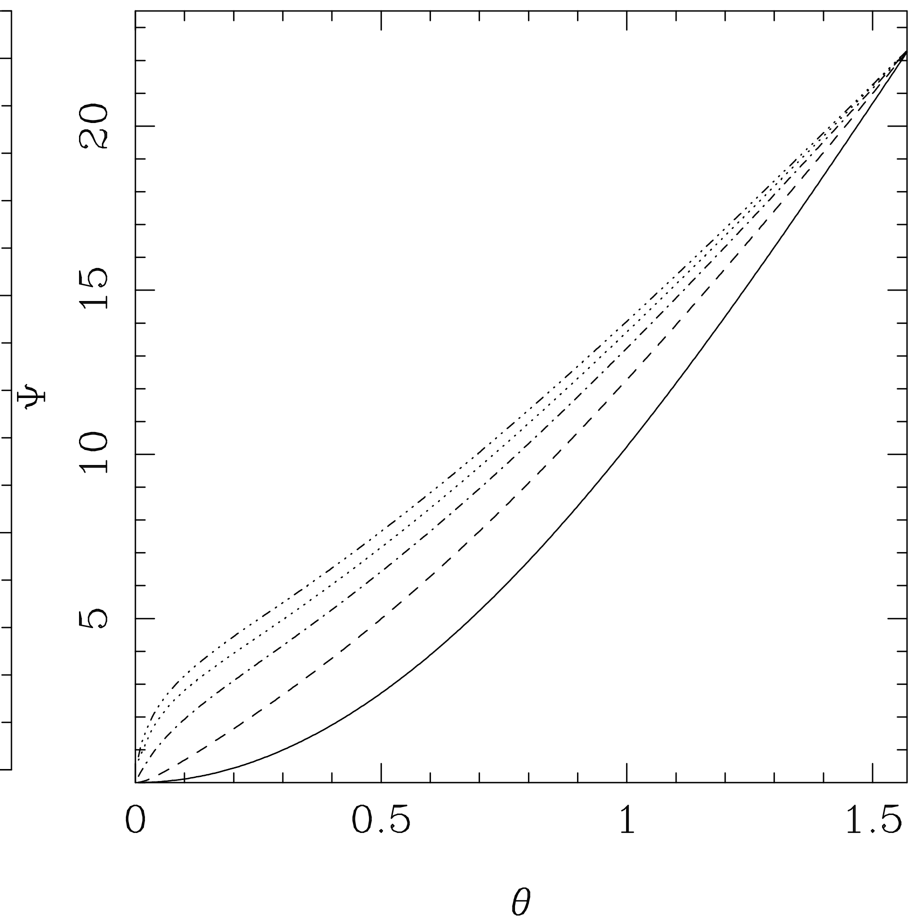

e.g. for $\Psi = 10$, $\vartheta = 57^{\rm o} \rightarrow 40^{\rm o}$
while for $\Psi = 5$, $\vartheta = 40^{\rm o} \rightarrow 15^{\rm o}$

Simulations of relativistic GRB jets

Komissarov, Vlahakis, Königl, & Barkov, in preparation

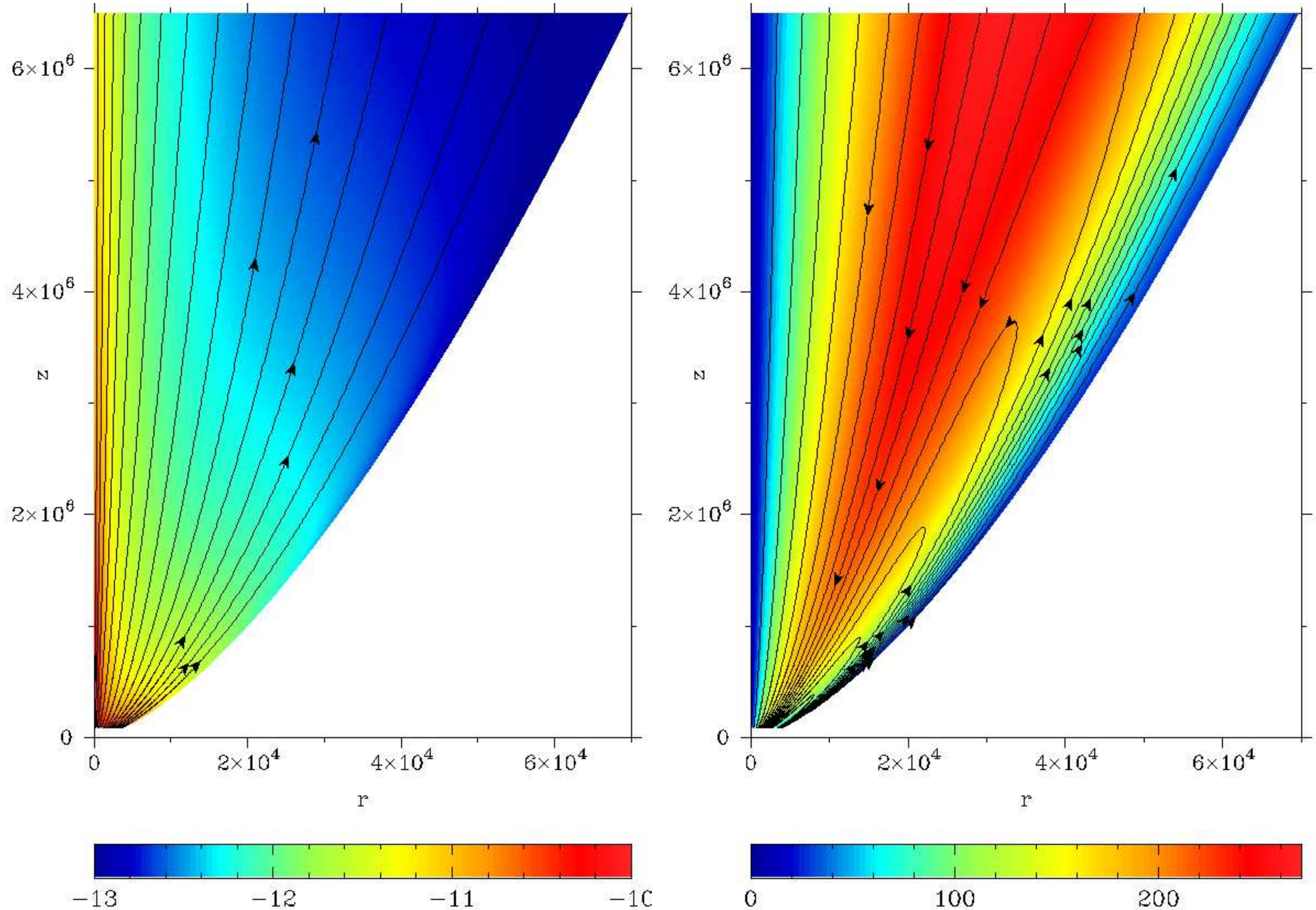

left: density/field lines, right: Lorentz factor/current lines (wall shape $z \propto r^{1.5}$)

Differential rotation → slow envelope

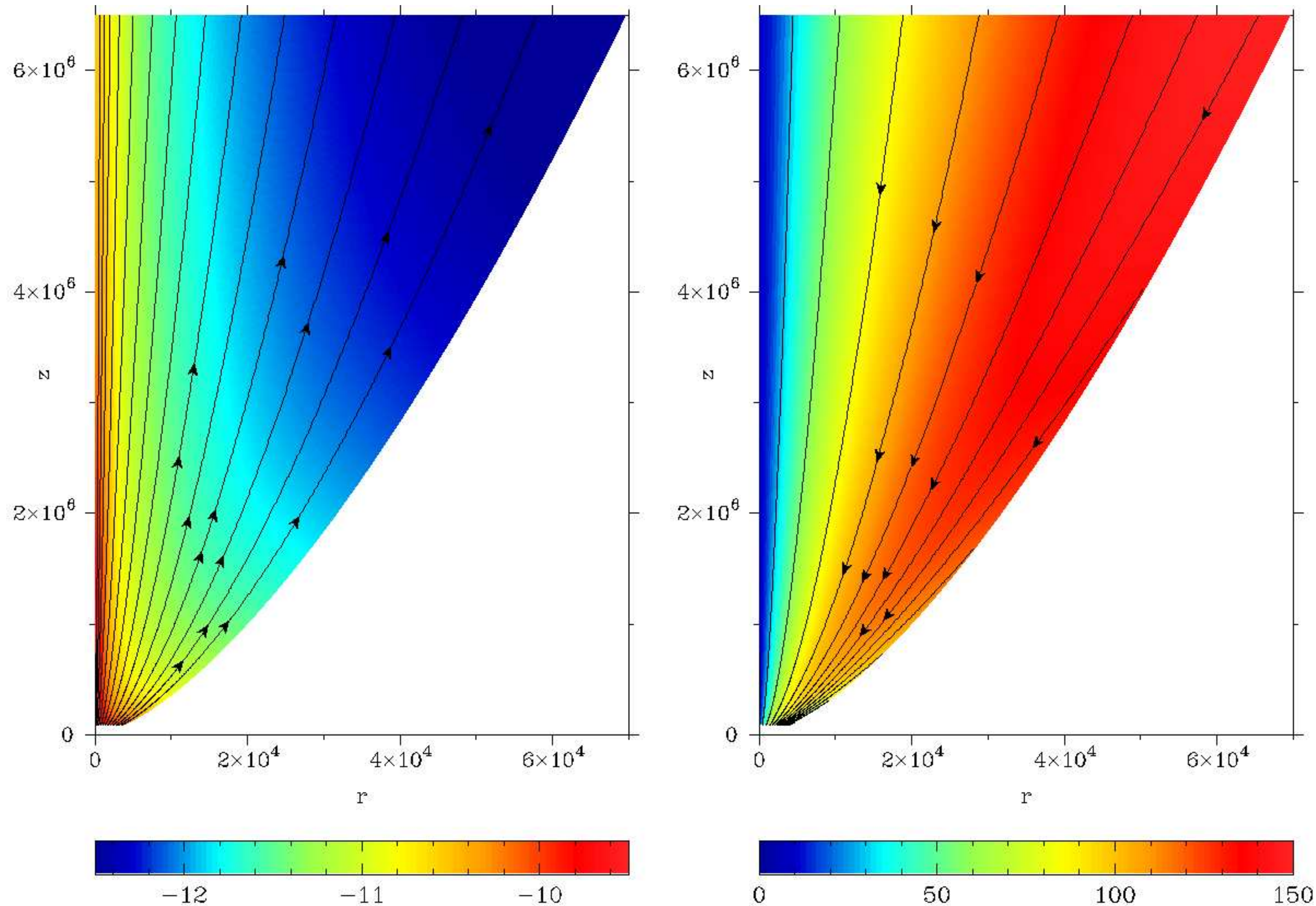

Uniform rotation $\rightarrow \gamma$ increases with r

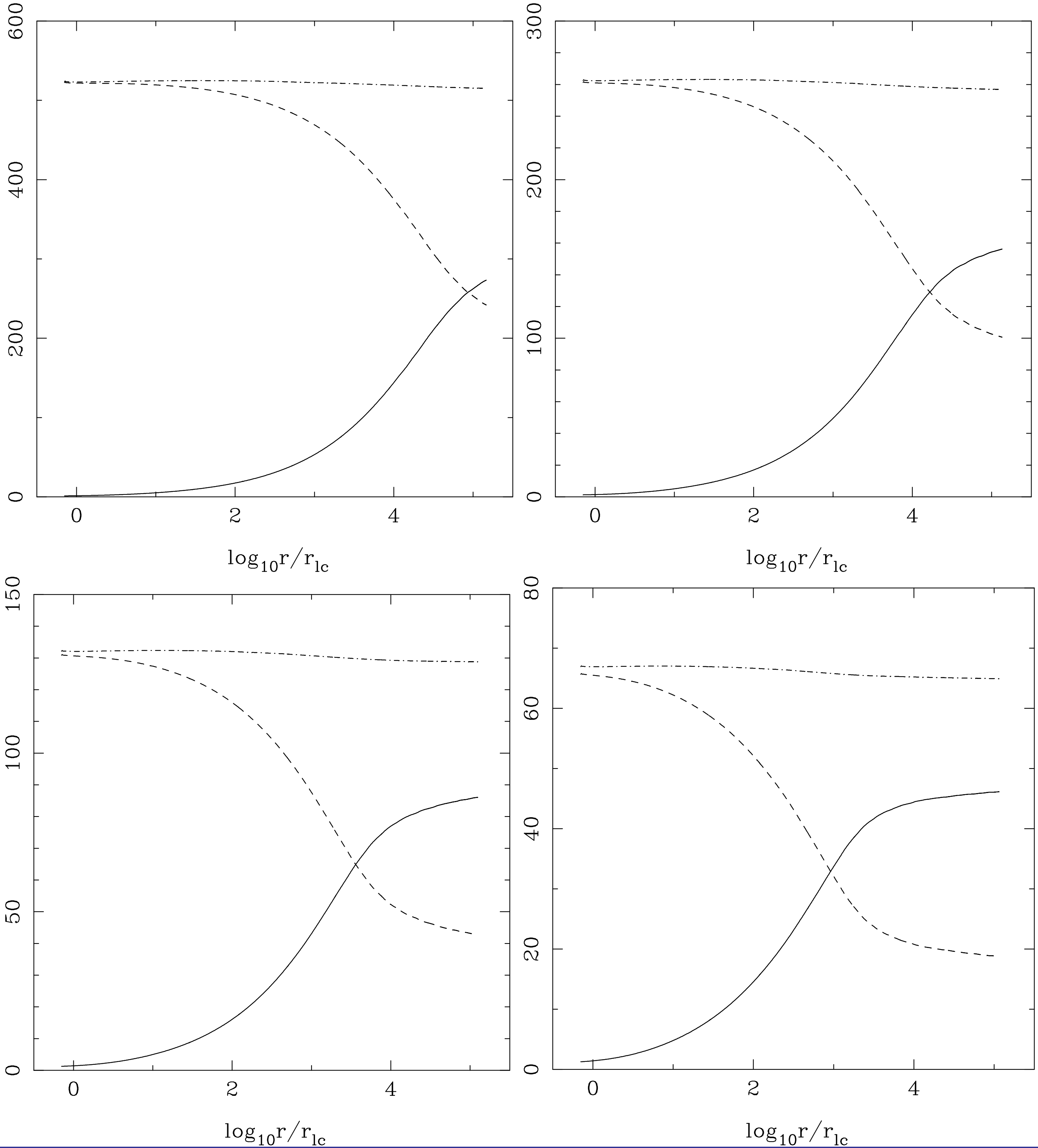

0
200
400
600
0
2
4
$\log_{10} r/r_{lc}$
0
100
200
300
0
2
4
$\log_{10} r/r_{lc}$
0
50
100
150
0
2
4
$\log_{10} r/r_{lc}$
0
20
40
60
80
0
2
4
$\log_{10} r/r_{lc}$

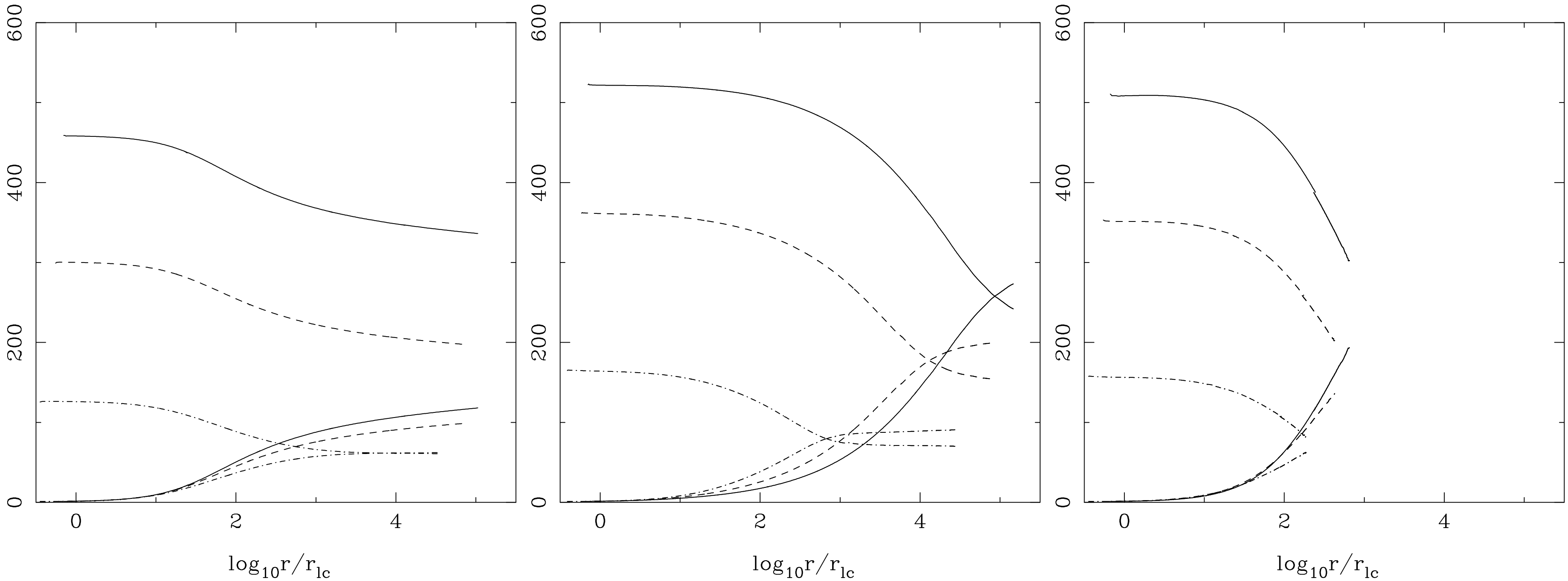

γ and $\gamma\sigma$ for wall-shapes:
$z \propto r$ (left), $z \propto r^{1.5}$ (middle), $z \propto r^2$ (right)

In the conical $\gamma \sim r\Omega/c$, but small efficiency

In parabolic, Lorentz factor $\gamma \sim z/r \propto r^{1/2} \propto R^{1/3}$ (middle)
and $\gamma \sim z/r \propto r \propto R^{1/2}$ (right)
efficiency $\sim 50\%$

$B_p \varpi^2/(2A)$

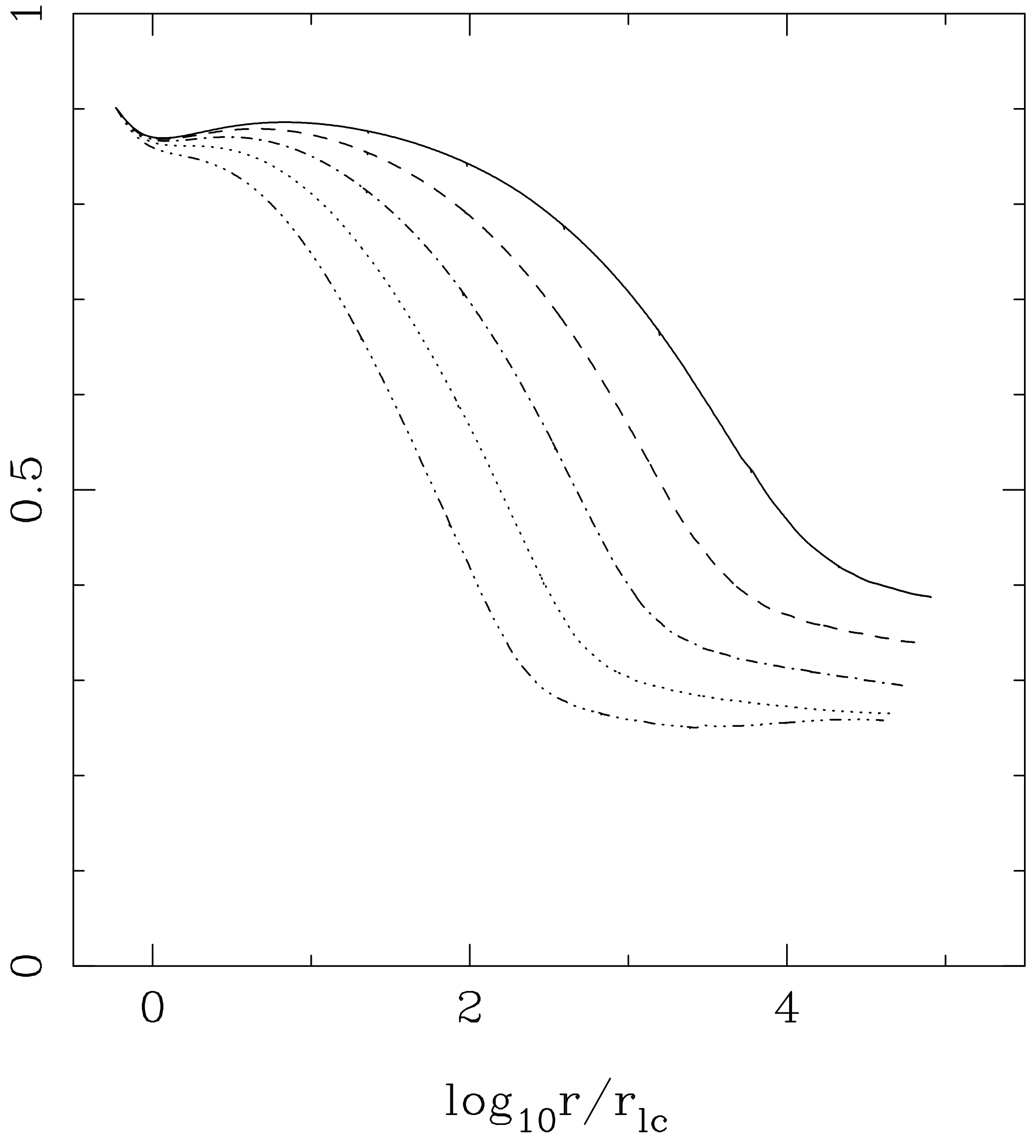

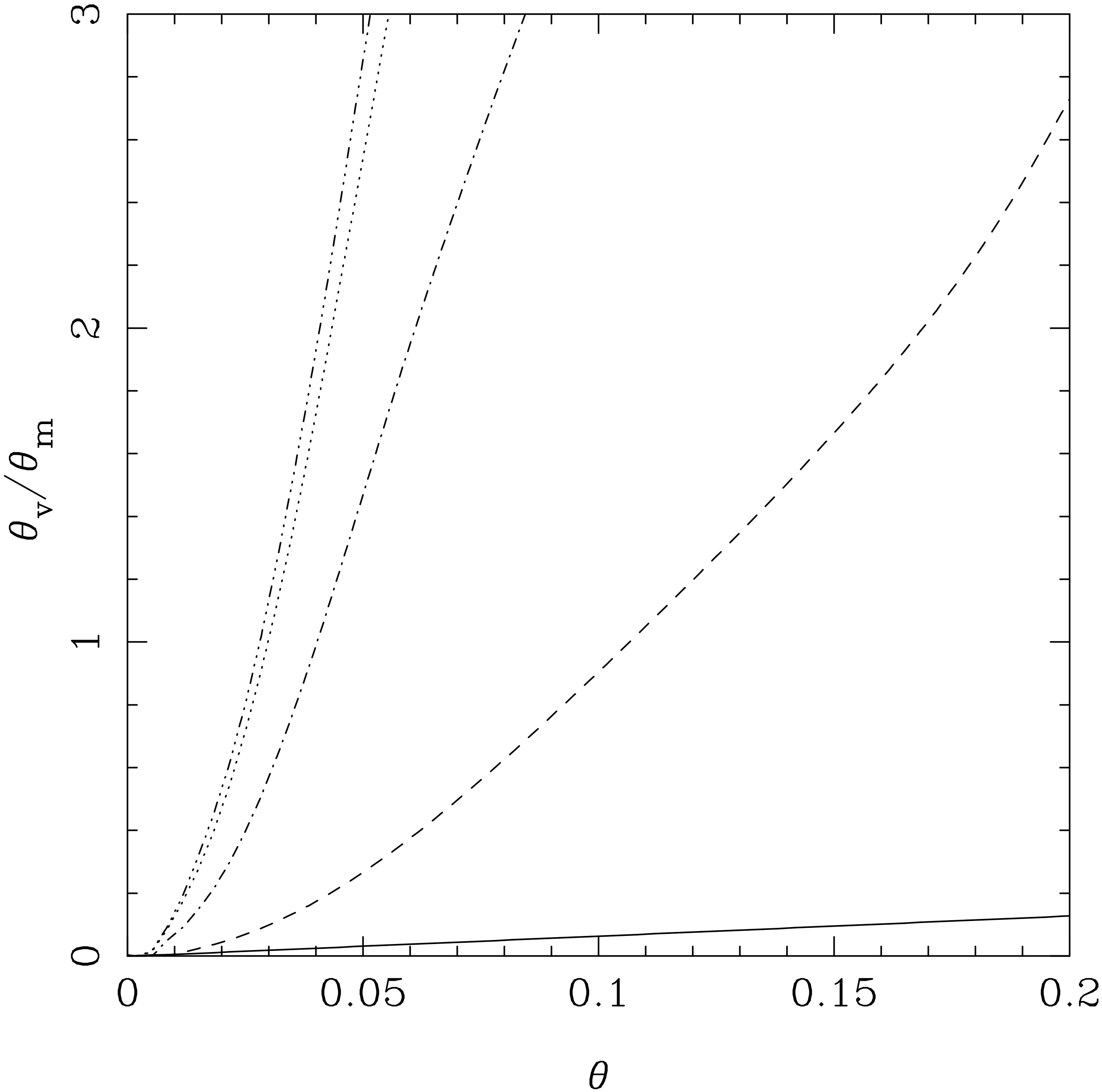

θ_v/θ_m
0
1
2
3
0
0.05
0.1
0.15
0.2
θ

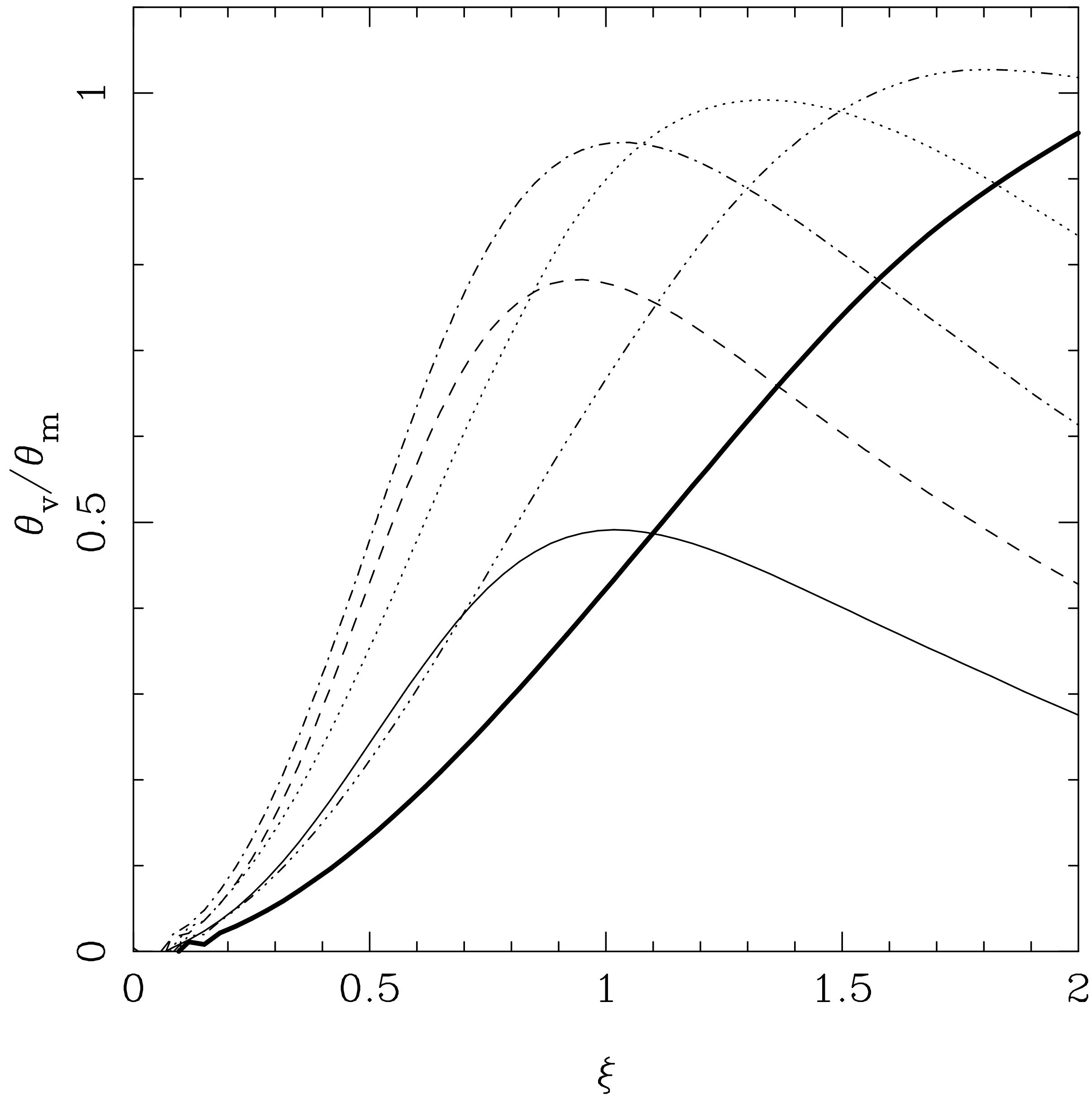

causal connection → collimation → acceleration

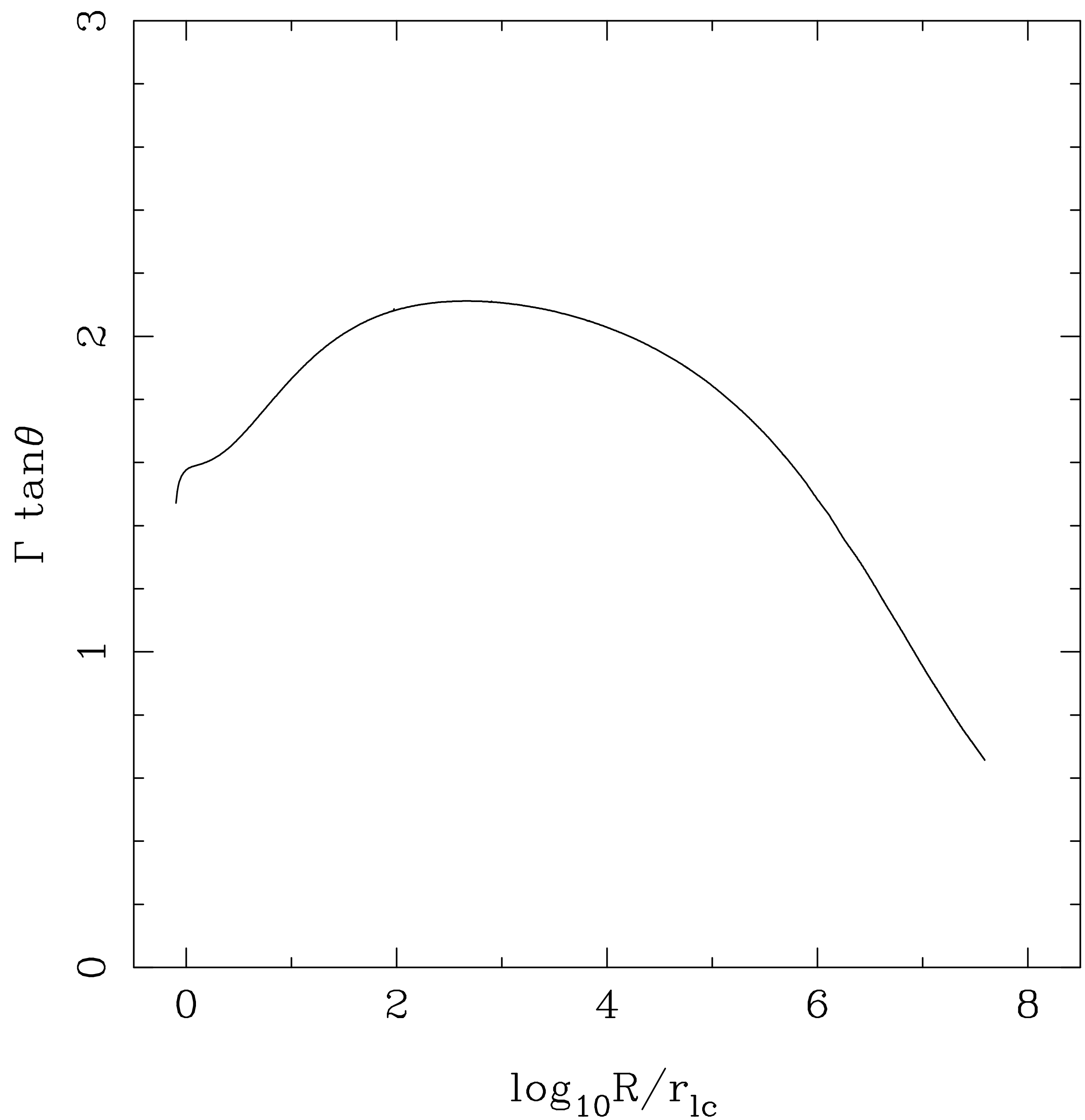

$\gamma \sim dz/dr \sim$ 1/(half-opening angle)

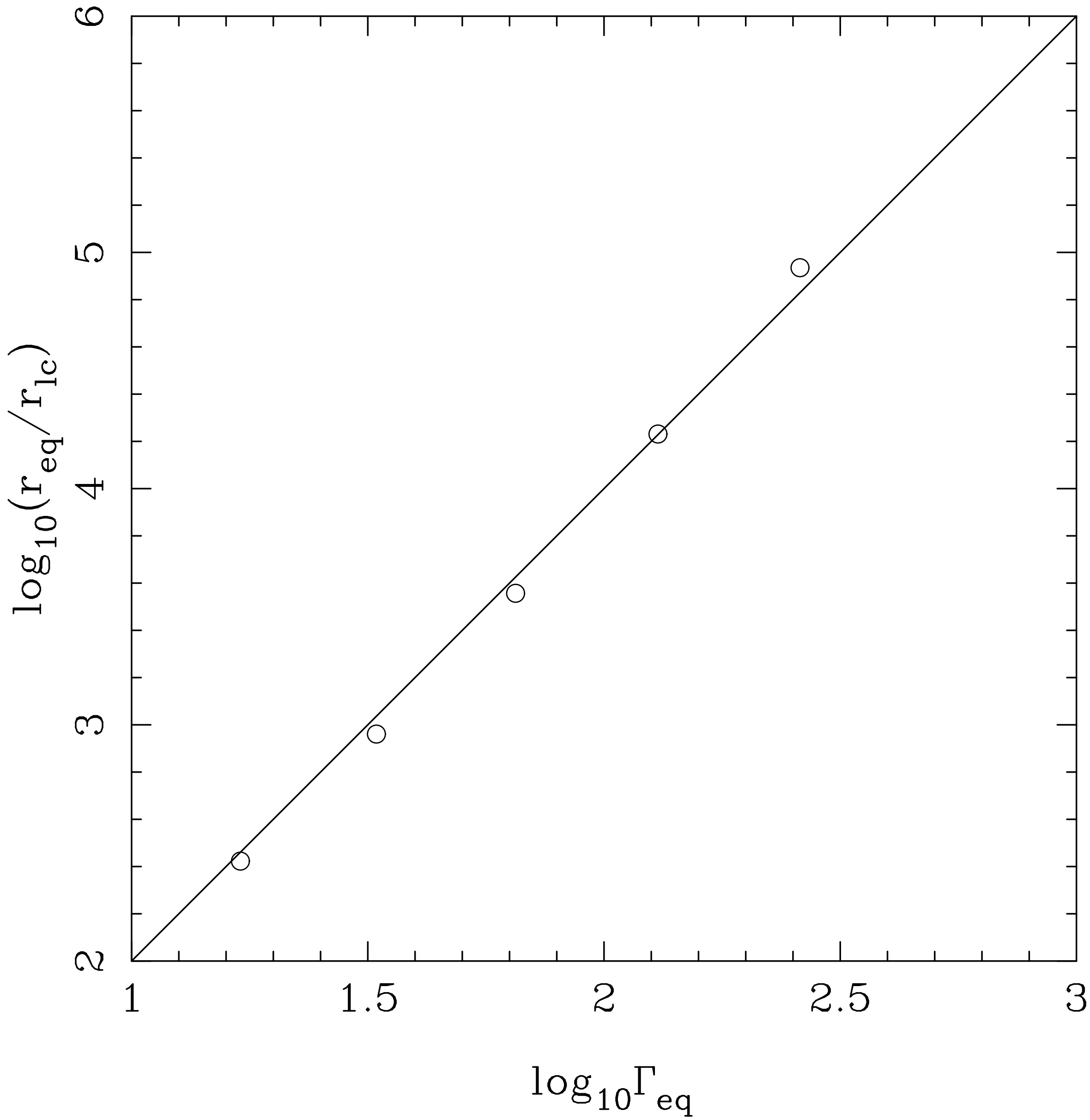

$$\gamma \sim (r/r_{\rm lc})^{1/2} \rightarrow \mu/2 \sim (r_{\rm eq}/r_{\rm lc})^{1/2} \rightarrow r_{\rm eq} \sim (\mu/2)^2 r_{\rm lc}$$

where μ = energy/ mass c^2

(μ = maximum Lorentz factor)

Summary

⋆ MHD could explain the dynamics of relativistic jets:

- acceleration (the flow is initially thermally, and subsequently magnetically accelerated up to Lorentz factors corresponding to rough equipartition between kinetic and Poynting fluxes)
  $\gamma_\infty \approx 0.5 \frac{\mathcal{E}}{Mc^2}$
- collimation
  parabolic shape $z \propto \varpi^{\beta+1}$ consistent with $\gamma \sim z/\varpi \propto \varpi^{\beta}$

⋆ The paradigm of MHD jets works in a similar way in all astrophysical jets

Angular momentum extraction

$$L = \mu\Omega{\varpi_{\mathrm{A}}}^2 \text{ where } \mu = \frac{\frac{dE}{dSdt}}{\frac{dM}{dSdt}c^2} = \text{maximum Lorentz factor}$$

So rate of angular momentum $= \mu\Omega\varpi_{\mathrm{A}}^2\dot{M}_j$ (initially carried by the field and later by the matter).

In the disk, rate $= \Omega\varpi_0^2\dot{M}_a$. If these are equal, $\frac{\dot{M}_j}{\dot{M}_a} = \frac{\varpi_0^2}{\mu\varpi_{\mathrm{A}}^2}$.

- in YSO confirmed by HST observations! (Woitas et al 2005)
- in GRBs $\dot{M}_a = 0.01 M_\odot s^{-1}\left(\frac{\dot{M}_j}{10^{-6}M_\odot s^{-1}}\right)\left(\frac{\mu}{400}\right)\left(\frac{\varpi_{\mathrm{A}}/\varpi_0}{5}\right)^2$

  (cf Popham et al 1999)

  (This is equivalent to $\frac{dE}{dt} \equiv \mu\dot{M}_j c^2 = \frac{GM\dot{M}_a}{\varpi_0}$.)

Jet kinematics

- due to precession? (e.g., Caproni & Abraham)
- instabilities? (e.g., Hardee, Meier)

bulk jet flow may play at least a partial role

to explore this possibility, we used the relativistic self-similar model (Vlahakis & Königl 2004)

since the model gives the velocity (3D) field, we can follow the motion of a part of the flow

For given $\theta_{\rm obs}$ (angle between jet axis and line of sight) and ejection area on the disk (r_o, ϕ_o), we project the trajectory on the plane of sky and compare with observations. Find the best-fit parameters r_o, $\theta_{\rm obs}$, ϕ_o.

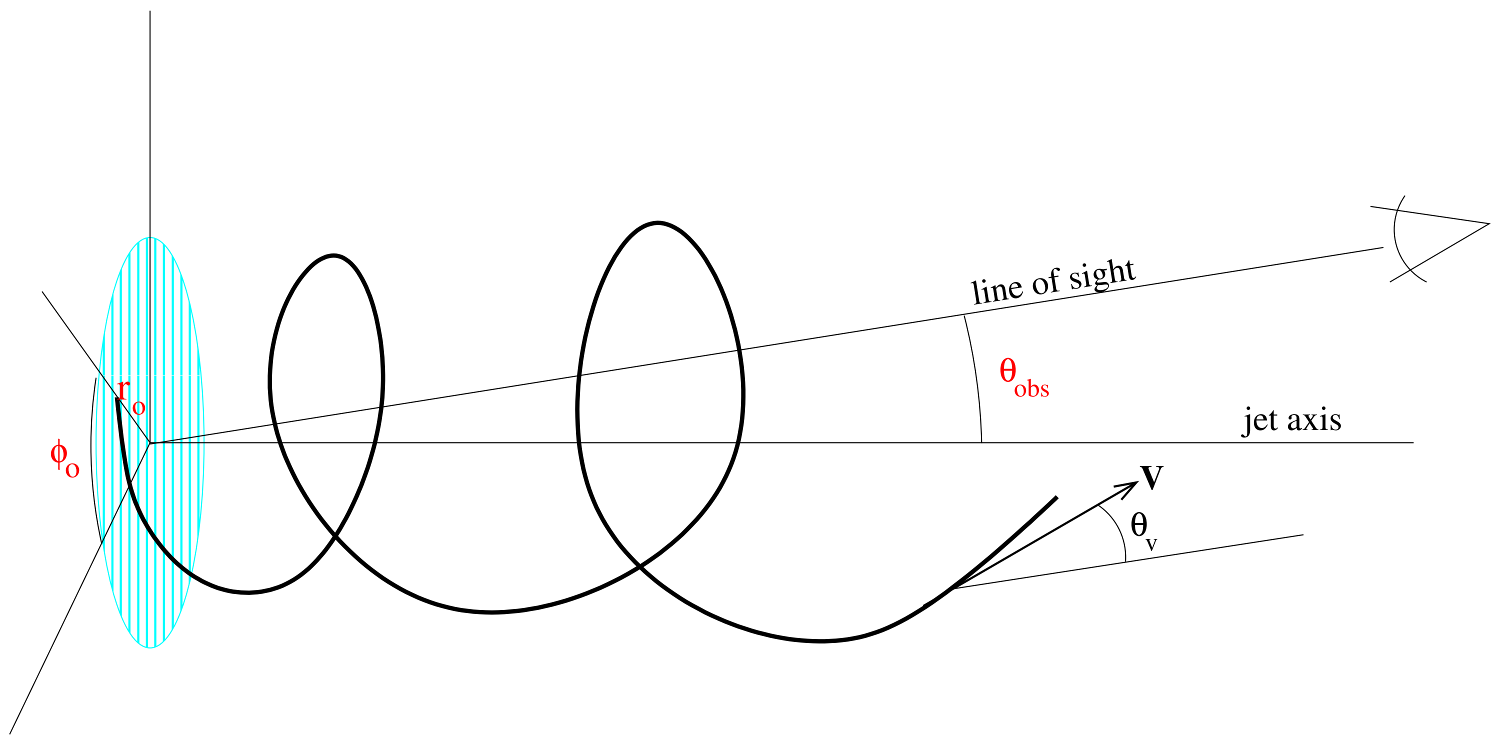

Preliminary results (Vlahakis & Königl in preparation)

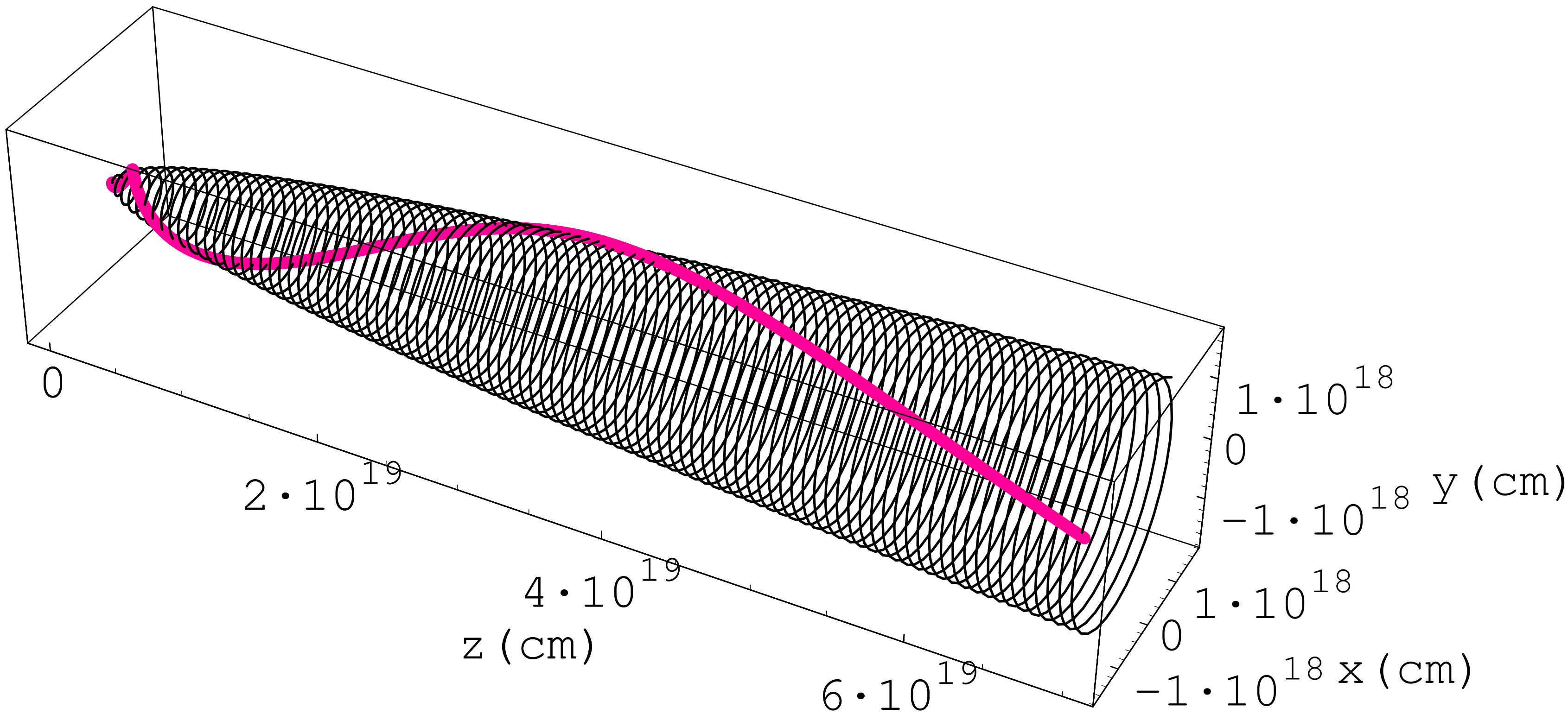

best-fit to Unwin et al results for C7 component in 3C 345:

$r_o \approx 2\times10^{16}$cm, ϕ_o=180^o and $\theta_{\rm obs}$=9^o

apparent trajectory

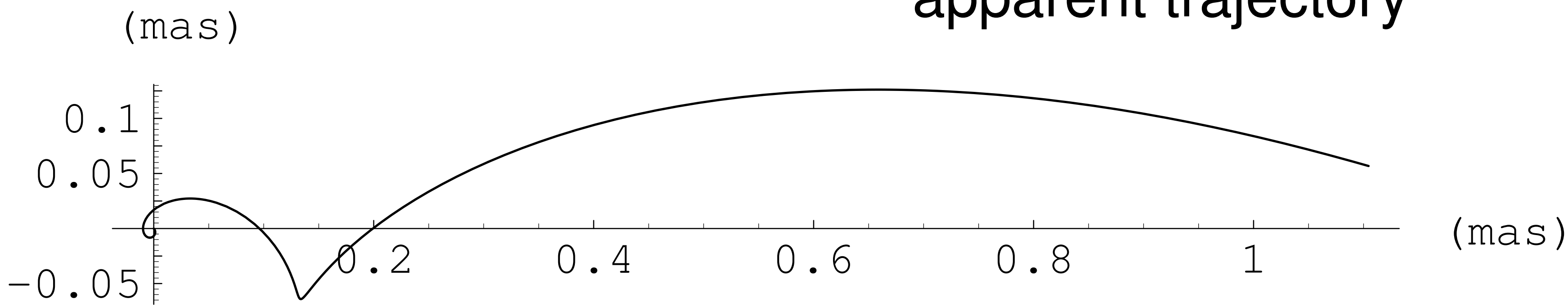

Trajectory of C7

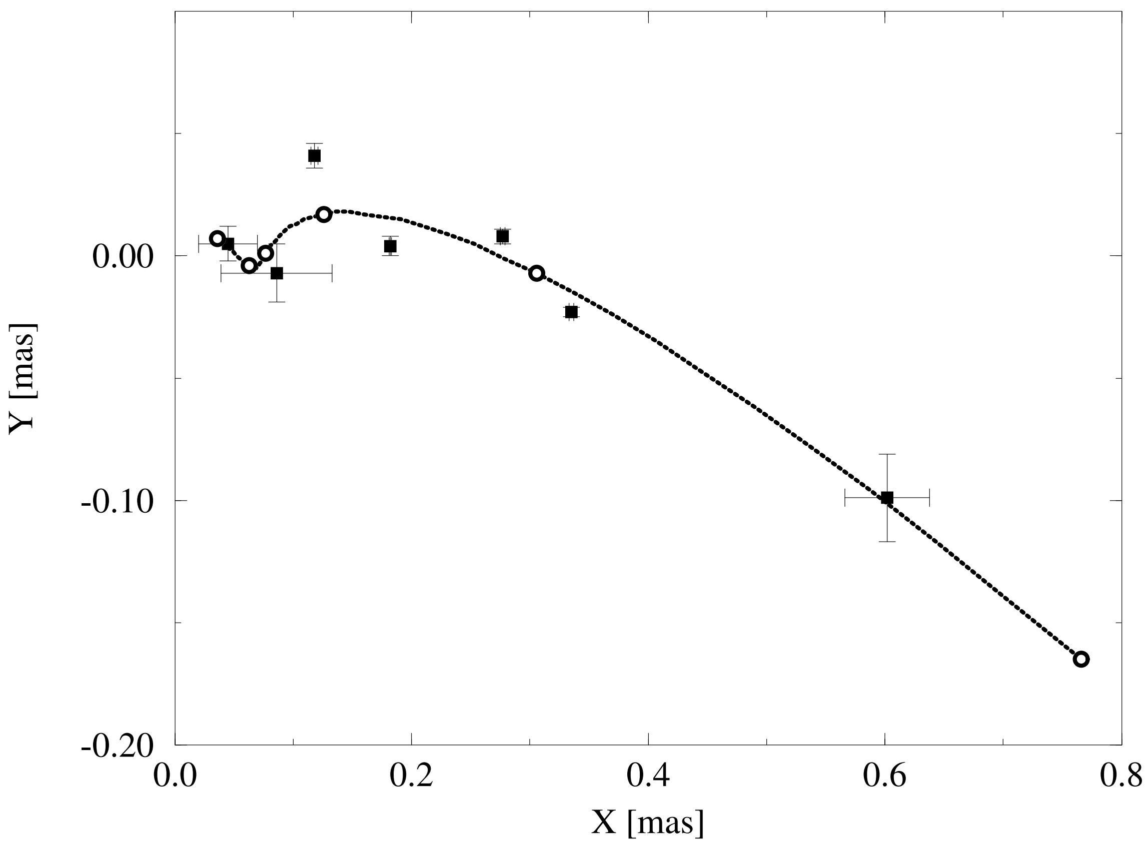

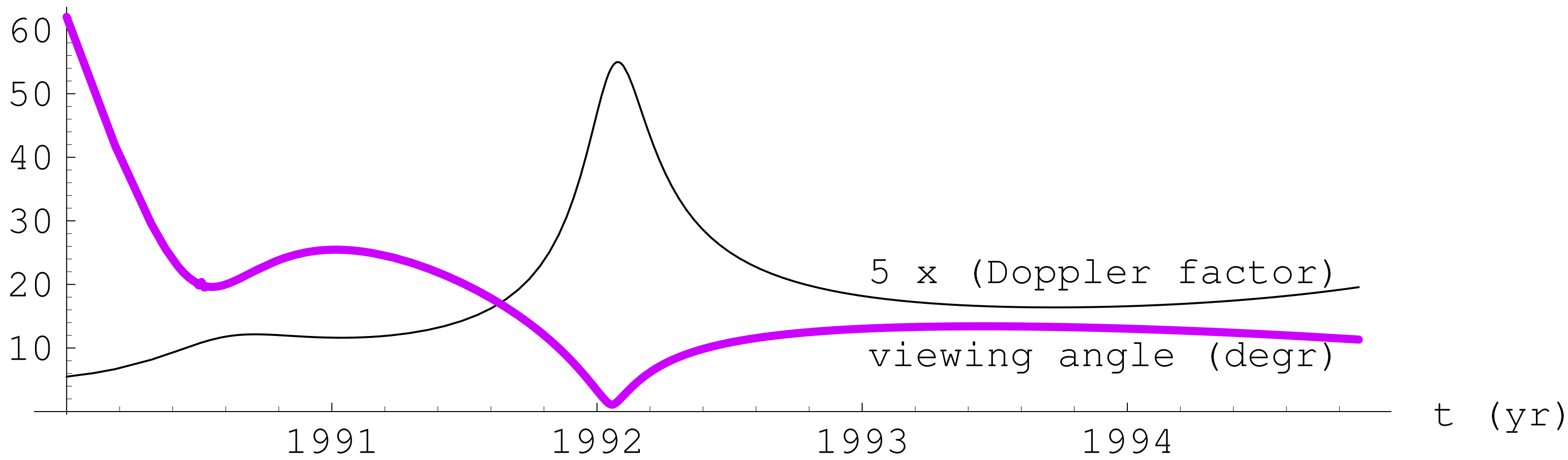
60
50
40
30
20
10
5 x (Doppler factor)
viewing angle (degr)
1991
1992
1993
1994
t (yr)

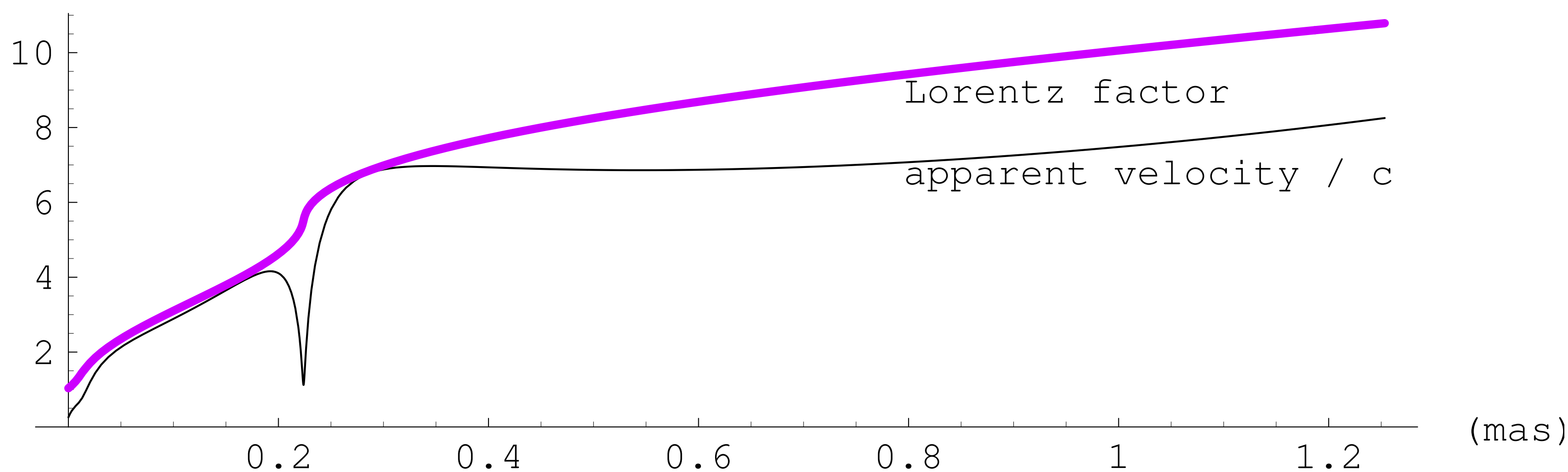
10
8
6
4
2
Lorentz factor
apparent velocity / c
0.2
0.4
0.6
0.8
1
1.2
(mas)

Polarization maps

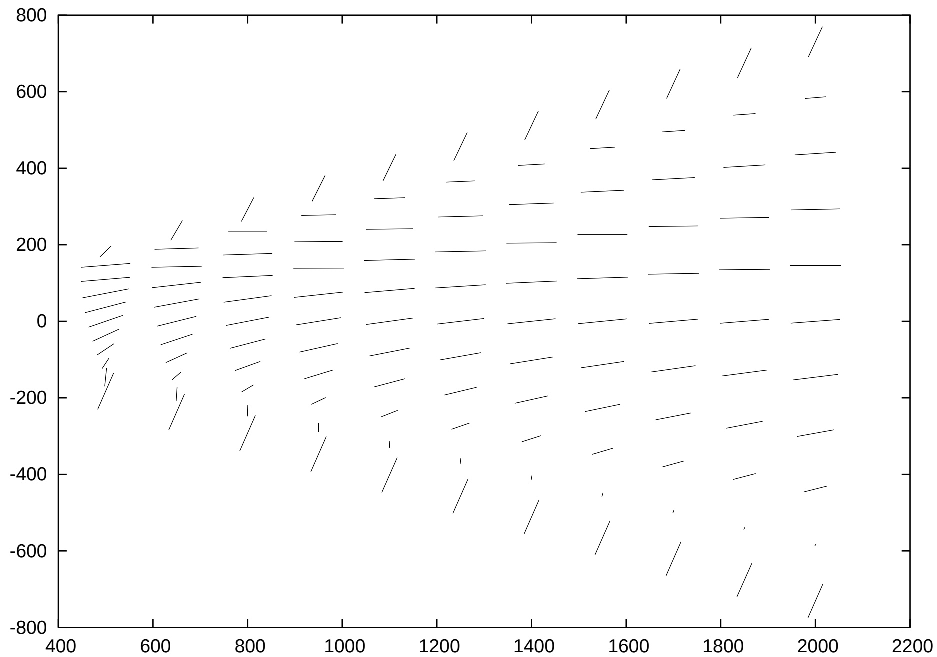

$\gamma = 10$, $\theta_{obs} = 1/2\gamma$, jet half-opening=1 degree, pitch angle at a reference diastance = 0.1 degrees
electron's energy spectrum $\propto \gamma_e^{-2.4}$

Polarization maps

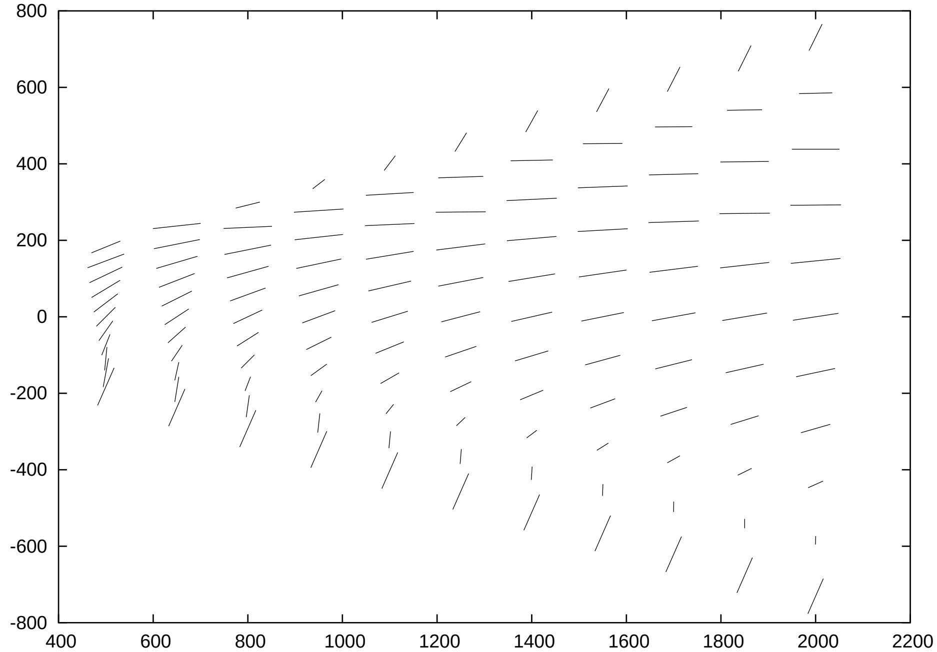

$\gamma = 10$, $\theta_{obs} = 1/2\gamma$, jet half-opening=1 degree, pitch angle at a reference diastance = 0.05 degrees
electron's energy spectrum $\propto \gamma_e^{-2.4}$